

Master Thesis in Geosciences

# Drill parameter analysis in the Løren tunnel

*Normalization and interpretation of automatically  
collected borehole data*

**Jonas Gjerstad Hjelle**



**UNIVERSITY OF OSLO**

**FACULTY OF MATHEMATICS AND NATURAL SCIENCES**



# Drill parameter analysis in the Løren tunnel

*Normalization and interpretation of automatically collected  
borehole data*

Jonas Gjerstad Hjelle



Master Thesis in Geosciences

Discipline: Geohazards and engineering geology

Department of Geosciences

Faculty of Mathematics and Natural Sciences

UNIVERSITY OF OSLO

June 1st. 2010

© **Jonas Gjerstad Hjelme, 2010**

Tutors: Ph.D. Vidar Kveldsvik

Professor Arild Andresen

This work is published digitally through DUO – Digitale Utgivelser ved UiO

<http://www.duo.uio.no>

It is also catalogued in BIBSYS (<http://www.bibsys.no/english>)

All rights reserved. No part of this publication may be reproduced or transmitted, in any form or by any means, without permission.

# Abstract

During the last decades, the Norwegian method of tunneling has been reviewed and continuously updated with the latest information and research results available. Despite the effort of making the practice of tunnel construction as efficient and safe as possible, the analysis of drill response parameters has not yet become a standard in the field.

The use of drill parameter response in underground openings and tunnels is a helpful tool in assessing information on structural and mineralogical features. When drilling in hard rock with rotary percussive drilling, the drill data are in most cases automatically collected, but hardly analyzed.

In this study drill parameters collected in the Løren tunnel, a road tunnel surrounding central Oslo, Norway, have been normalized and compared to engineering geological mapping collected by on site engineering geologists.

The normalization process itself has been evaluated regarding the sensitivity and reliability of the method and the normalized parameters have been put to test. Results show that normalized drill parameters such as penetration rate and torque pressure respond to changing rock conditions, but the sensitivity of the normalization process is high and measures has to be taken in order to use single drill parameters for rock characterization. Also research of the penetration rates dependency to uniaxial compressive strength has been evaluated and a relationship has been found.

## Acknowledgements

First of all I would like to thank my supervisor Vidar Kveldsvik at NGI for giving me the possibility to write this thesis and for reviews and feedbacks. I would also like to thank Jørgen Stenerud at Statens Vegvesen for supplying the data and for answering numerous emails. Rolf Elsrud at Atlas Copco AB is an excellent problem solver and has helped me a lot with understanding the features of Tunnel Manager along with professor Håkan Schunnesson who's emails have been of good help. Thorvald Wetlesen at Bever Control, thank you for the inputs.

A special thank to Nils Tarjei Hjelme for helping me out with his programming skills.

The "study desk gang" Anders, Eirik, Jonas and Christian for making late nights at the university manageable with both scientifically and unscientifically joyful discussions and pleasant coffee breaks.

Last but not least, a big thanks to my family for supporting me throughout the years as a student, and especially Anette Borge for keeping up with me the last couple of months.

# Table of Contents

- ABSTRACT.....5**
- ACKNOWLEDGEMENTS.....6**
- TABLE OF CONTENTS.....7**
  - LIST OF FIGURES .....10
  - LIST OF TABLES.....12
- 1. INTRODUCTION.....13**
  - 1.1 BACKGROUND .....13
  - 1.2 DRILL MONITORING .....14
  - 1.3 PROBLEM DEFINITION AND OBJECTIVES .....15
- 2. THEORETICAL BACKGROUND .....16**
  - 2.1 GEOLOGICAL SETTING.....16
  - 2.2 THE DRILL RIG .....18
  - 2.3 PARAMETERS AND DRILLABILITY .....20
    - 2.3.1 *Earlier research*.....20
    - 2.3.2 *Drill parameters* .....21
  - 2.4 TUNNEL MANAGER MWD.....23
  - 2.5 NORMALIZATION OF BOREHOLE PARAMETERS .....23
  - 2.6 ROCK QUALITY DESIGNATION AND THE Q-METHOD .....25
  - 2.7 RQD PREDICTION IN DRILL MONITORING .....26
- 3. METHODOLOGY AND DATASETS .....27**
  - 3.1 DRILL DATA IN THE LØREN TUNNEL.....27
  - 3.2 DRILL EQUIPMENT IN THE LØREN TUNNEL .....28

3.3	VISUAL VERIFICATION OF TUNNEL MANAGER MODELS .....	28
3.4	PROGRAM FOR CALCULATED AVERAGE.....	29
3.5	NORMALIZATION PROCESS FOR BOREHOLE DEPTH .....	30
3.6	NORMALIZATION PROCESS FOR FEED THRUST .....	31
3.7	NORMALIZATION PROCESS FOR PENETRATION RATE DEPENDENT TORQUE AND TORQUE DEPENDENT PENETRATION RATE.....	31
3.8	INSPECTION OF NORMALIZED PARAMETERS.....	32
3.9	TEST OF ROCK HARDNESS VS PENETRATION RATE .....	32
<b>4.</b>	<b>RESULTS.....</b>	<b>34</b>
4.1	THE NORMALIZATION PROCESS .....	34
4.1.1	<i>Normalization for borehole depth.....</i>	<i>34</i>
4.1.2	<i>Normalization for feed thrust.....</i>	<i>37</i>
4.1.3	<i>Normalization of torque and penetration rate .....</i>	<i>38</i>
4.1.4	<i>Sample of normalized borehole data .....</i>	<i>39</i>
4.2	GEOMECHANICAL INTERPRETATION.....	40
4.2.1	<i>Chainage A1386 .....</i>	<i>40</i>
4.2.2	<i>Chainage A1442 .....</i>	<i>43</i>
4.2.3	<i>Chainage A1453 .....</i>	<i>46</i>
4.2.4	<i>Chainage B1378 .....</i>	<i>49</i>
4.2.5	<i>Chainage B1476 .....</i>	<i>52</i>
4.3	TESTED ROCK HARDNESS VS PENETRATION RATE .....	55
<b>5.</b>	<b>DISCUSSION .....</b>	<b>56</b>
5.1	THE NORMALIZATION PROCESS .....	56
5.1.1	<i>General sensitiveness of normalization process .....</i>	<i>56</i>
5.1.2	<i>Normalization for borehole depth.....</i>	<i>56</i>

5.1.3	<i>Normalization for feed thrust</i> .....	58
5.1.4	<i>Normalization for torque and penetration rate</i> .....	59
5.2	DISCUSSION OF GEOMECHANICAL INTERPRETATION RESULTS .....	59
5.2.1	<i>Chainage A1386</i> .....	59
5.2.2	<i>Chainage A1442</i> .....	60
5.2.3	<i>Chainage A1453</i> .....	61
5.2.4	<i>Chainage B1378</i> .....	62
5.2.5	<i>Chainage B1476</i> .....	62
5.2.6	<i>Tested rock hardness vs penetration rate</i> .....	63
5.3	REMARKS ABOUT COLLECTED DRILL MONITORING DATA .....	64
<b>6.</b>	<b>CONCLUSIONS</b> .....	<b>65</b>
<b>7.</b>	<b>REFERENCES</b> .....	<b>66</b>
	<b>APPENDIX I: ENGINEERING GEOLOGICAL MAPPING</b> .....	<b>68</b>
	<b>APPENDIX II: CD</b> .....	<b>74</b>

# List of figures

Figure 2.1. Geology in the Oslo region with tunnel position (modified from NGU 2010).\_\_\_\_\_ 16

Figure 2.1 Drawing of typical percussive top-hammer drill (from Thuro 1997)\_\_\_\_\_ 18

Figure 3.2. Demonstration of how the regression line is modified for borehole depth\_\_\_\_\_ 30

Figure 4.1. Calculated averages from injection holes (left), and blast holes (right). Data outside the red lines are ignored in the regression calculation. \_\_\_\_\_ 34

Figure 4.2. Modified averages with regression. \_\_\_\_\_ 35

Figure 4.4. Averaged penetration rate and torque pressure plotted against feed thrust for injection holes (left) and blast holes (right). The parameters are normalized for borehole length. Blue lines are locally weighted scatterplot smoothing (LOWESS) fit for the averaged data, and the red dotted lines the linear regression lines. \_\_\_\_\_ 37

Figure 4.5. Regression lines for torque pressure and penetration rate. All parameters are normalized for borehole depth variation and feed thrust variation. Left side injection holes, right side blast holes. The blue line represent a LOWESS fit of the data and the red dotted lines represent the linear regression. \_\_\_\_\_ 38

Figure 4.6. Raw and normalized torque pressure from chainage A1442 injection hole 46. The data are modified with floating average for easier comparison. \_\_\_\_\_ 39

Figure 4.6. Location of boreholes -53 and -49. Section from chainage A1386 \_\_\_\_\_ 40

Figure 4.7. Normalized torque pressure and penetration rate for chainage A1386 holes -49 and -53 \_\_\_\_\_ 41

Figure 4.8. Calculated fracturing and hardness mapping (left), and calculated fracturing and hardness in boreholes (right) from chainage A1386. All images and parameters generated by Tunnel Manager. \_\_\_\_\_ 42

Figure 4.7. Location of boreholes 46 and -58. Section from chainage A1442. \_\_\_\_\_ 43

Figure 4.8. Normalized penetration rate and torque pressure for chainage A1442 holes 46 and -58 \_\_\_\_\_ 44

Figure 4.9. Calculated fracturing and hardness mapping (left), and calculated fracturing and hardness in boreholes (right) in chainage A1442. All images and parameters generated by Tunnel Manager. \_\_\_\_\_ 45

<i>Figure 4.13. Location of boreholes -17 and -14. Section from chainage A1453.</i>	46
<i>Figure 4.14. Normalized penetration rate and torque pressure from chainage A1453, holes -14 and -17</i>	47
<i>Figure 4.15. Calculated fracturing and hardness mapping (left), and calculated fracturing and hardness in boreholes (left) from chainage A1453. All images and parameters generated by Tunnel Manager.</i>	48
<i>Figure 4.16. Location of boreholes -20 and -17. Section from chainage B1378.</i>	49
<i>Figure 4.17. Normalized torque pressure and penetration rate for chainage B1378, holes -20 and -17</i>	50
<i>Figure 4.18. Calculated fracturing and hardness mapping (left), and calculated fracturing and hardness in boreholes (left) from chainage B1378. All images and parameters generated by Tunnel Manager.</i>	51
<i>Figure 4.19. Location of boreholes -15 and 28. Section from chainage B1476.</i>	52
<i>Figure 4.20. Normalized torque pressure and penetration rate from chainage B1476, holes -15 and 28.</i>	53
<i>Figure 4.21. Calculated fracturing and hardness mapping (left), and calculated fracturing and hardness in boreholes (right) from chainage B1476. All images and parameters generated by Tunnel Manager.</i>	54
<i>Figure 4.22. Average blast borehole penetration rates for shale, limestone and syenite. Data are normalized for borehole depth.</i>	55
<i>Figure 5.1. Number of averaged data plotted against reading number. Red lines indicate the where the threshold should be placed regarding amount of data.</i>	57
<i>Figure 5.2. Scatterplot of torque pressure and penetration rate with marked threshold. All data are normalized for borehole depth and feed thrust</i>	59

# List of tables

*Table 3.1 The mechanical properties of different rock types found in drill cores in the Løren tunnel. (modified from Haug et al. 2007)* \_\_\_\_\_ 27

*Table 4.1. Equations for regression lines in Figure 4.2.* \_\_\_\_\_ 36

*Table 4.2 Equations for regression lines in Figure 4.4.* \_\_\_\_\_ 37

*Table 4.3. Equations for regression lines in Figure 4.5.* \_\_\_\_\_ 38

*Table 4.4. Average penetration rate normalized for depth and UCS for syenite, limestone and shale* \_\_\_\_\_ 55

# List of equations

*Equation 2.1* \_\_\_\_\_ 25

# 1. Introduction

## 1.1 Background

The Løren tunnel project is a road tunnel part of Oslopakke 2 financed by the Norwegian Ministry of Transport and Communication. The tunnel will increase the transport capacity on the Ring 3, a highway surrounding central Oslo, and is to be finished during the year 2013 (Haug et al. 2007).

The main tunnel line is about 1200 meters, with 915 meters running through rocks (Statens\_Vegvesen 2009). The two tunnel lines have a spacing of 10 meters, which connects in the entrances. Haug et al. (2007) have searched the area above the tunnel for exposed bedrock, but there is literally none. The geology is explored by borehole tomography, drill cores and seismic refraction techniques. The area above the tunnel line is mostly covered with urban settlement and industrial buildings.

In Norway, the method of tunneling has been developed for road systems with moderate traffic density levels. The construction technique has focused on quick and cost effective excavation. Drill and blast has been the preferred technique, but also tunnel boring machine (TBM) drilling has been used.

Accidents and insecurity during construction and post construction in tunnel projects, as in the Hanekleiva and Romerikeporten in example, has weakened the confidence and reputation of the Norwegian method of tunneling.

This thesis is a part of the project “Tunnel Stability: Documentation and verification, DP2: *Verification of rock mass quality for tunnel support needs*” at the Norwegian Geotechnical Institute. The goal for the project is to further develop the methods of the Norwegian tunneling method by developing and verifying procedures for project planning, equipment and technology so that potential zones of weakness can be identified before or during construction.

The thesis is based upon drill parameters and engineering geological mapping collected in the Løren tunnel during 2009 and 2010. The drill rigs at the site automatically collect the drill parameters, and the engineering geological mapping is collected by on site engineering geologists.

## 1.2 Drill Monitoring

The process of drill monitoring has been available for the past decades as a tool designed for assessing information about geological features ahead the rock face in tunnel and mining practice, but has not yet become a standard in the industry (Schunnesson 1998). Actors in the tunneling industry are now working together on establishing a standard, IREDES. IREDES' goal is to standardize information exchange interface for rock excavation and mining equipment, so that computers and machinery can “talk” together without the help from individual software. Through the IREDES program, the process of drill monitoring can be even more accessible in the future.

The basis of drill monitoring is to understand the response drill parameters show upon drilling. Geological features as rock hardness and fracturing affect the drill parameters with it's own “signature”. However the most important parameters are highly dependent upon each other and one respond to changes in another. To successfully interpret geological features from drill parameter data, normalization of dependent parameters for other influential parameters are essential. However, normalization of drill data is highly dependent upon the trends in the data.

## 1.3 Problem definition and objectives

The main objectives in this are as follows:

- The effect on the results due to normalization with respect to borehole length and influential parameters: It will be analyzed how sensitive the results is to how this normalization is performed.
- Identify geological boundaries and zones of weakness through Tunnel Manager MWD and verify these through comparison of engineering geological maps.
- How well does the borehole parameters correlate with mechanical rock properties obtained from core drillings?

## 2. Theoretical Background

### 2.1 Geological setting

The Løren tunnel is situated north of Oslo city center, and the area is typical for the geology in the Oslo region, with mostly Cambro-Silurian sedimentary rocks, intruded with Permian igneous dykes dated to approximately 260-280 million years ago (Haug et al. 2007).

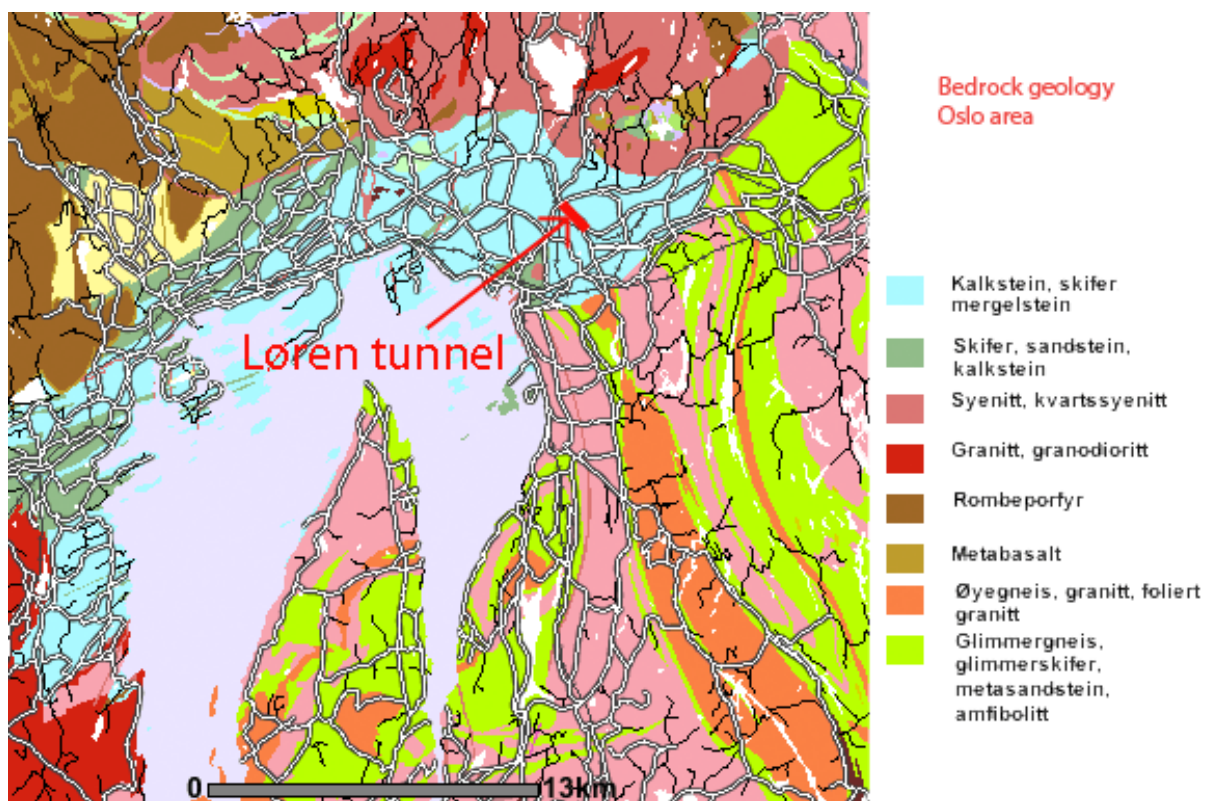


Figure 2.1. Geology in the Oslo region with tunnel position (modified from NGU 2010).

During the rifting episodes in the Carboniferous and Permian, 310 to 241 millions years ago, volcanic rocks intruded and covered most of the Cambro-Silurian sedimentary rocks in the region (Larsen et al. 2007). Later glaciations has removed parts of the covering volcanic rocks, and exposed the sedimentary rocks. Statens Vegvesen has drilled four core samples and 11 thin sections that are characteristic and important for the rock types have been examined with microscope and show a composition and mineralogy representative for the

Oslo region (Haug et al. 2007). The rocks observed in the core samples were clay shale, nodular limestone, dark shale, syenite, maenite, rhombic porphyry and diabase.

The sedimentary rocks are part of the “Elnes” formation dated back to Ordovician, 490 to 443 million years ago. Parts of the tunnel will also cross through sections of the “Vollen” formation, which are somewhat coarser and contain more sand than the “Elnes” formation. There are micas in all of the sedimentary rocks, but it is only in the dark shale that the micas are abundant enough and have a foliation axis that influences the strength of the rock. During the Caledonian orogeny the Scandian contraction created South-East directed fold axis (Andersen 1998), but there are local variations that show folding in N40-60°E (Haug et al. 2007).

The faulting that has occurred in the area shows zones of crushed rock in 1-3 centimeter thin planes with dip and strike equal to the folding axis. There are several deep-grooves in the area with large amounts of loose soil, the rock qualities under these trenches are assumed to be of much lower quality than in the rest of the area. Epidote fillings in cracks represents zones of weakness, and are usually developed from fault zones.

In general there are little clay in the core drillings, but it is assumed that there are more zones of swell clay in the area than discovered from the core drilling (Haug et al. 2007).

## 2.2 The drill rig

A typical rotary percussive drill usually consists of five main operating parts. A drill hammer, a shank adapter, a drifter rod, a drifter feed and a drill bit. The hydraulic drill hammer generates rotation and impact rate. The shank adapter connects the drifter rod to the drill hammer, and ensures maximum energy transmission. The drifter rod connects the drill bit and the shank adapter. The drifter feed that ensures the bit to have rock contact on each blow impact, and finally the drill bit that penetrates the rock through impacts generated by the drill hammer.

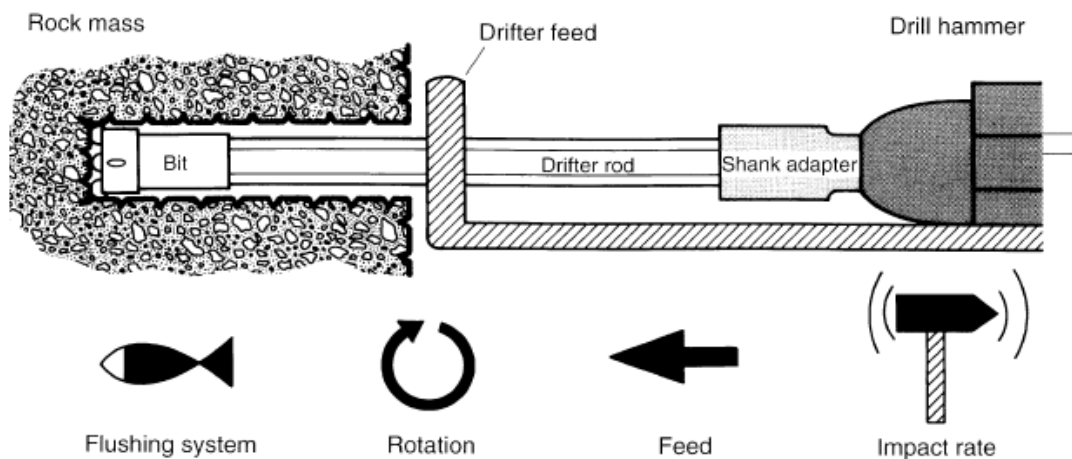


Figure 2.2 Drawing of typical percussive top-hammer drill (from Thuro 1997)

The top-hammer drill is used in most tunnel applications, and in contrast to in-the-hole drill hammers, the percussion and rotation is generated in the drill hammer outside the borehole, and not in the drill bit (Jimeno et al. 1995).

In large underground openings, as tunnels or caverns, the drill hammer is in most cases mounted on a drill rig. The drill rig is usually a wheel or belt driven machine that can carry one or more drill hammers. The drill rig also has a control unit where an operator can adjust, monitor and control the drilling process.

During drilling, a flushing medium is also applied to remove crushed rock debris in the bottom of the hole. The flushing medium is usually water or air, and is forced through the drill bit during the entire drilling process. The flushing medium does not only help on

removing crushed rock in the bottom of the hole, but also works as a lubricant between the drill rods and the rock walls in the borehole.

Compared to rotary drilling, where the turning action (rotation speed and pressure) leads to penetration, the percussive drilling relies mostly on the crushing of rock (Schunnesson 1997). For every blow, the drill bit is turned around and the next blow will impact a new fragment of rock. The rotary percussion borehole drilling technique is also much more rapid, and has shown results 3 to 10 times faster than rotary core drilling (Honer and Sherrell 1977). Due to the rapidness, the time-cost is much more favorable in rotary percussive drilling and due to the time saved many more holes can be drilled. The fact that the rotary percussive boreholes itself are parts of the construction work (as blast holes, grouting holes and rock anchoring holes), strengthen the advantages.

(Jimeno et al. 1995) also sums up the main advantages:

- It can be applied to any type of rock.
- It supports a wide range of borehole diameters.
- It is versatile and adapts well to different operations and is very mobile.
- It requires only one operator.
- It is easy to maintain.
- Low capital cost.

## 2.3 Parameters and drillability

### 2.3.1 Earlier research

The fact that different types of rock, respond differently on drilling has been known for quite some time (Howarth and Rowlands 1987, Hoseinie et al. 2007 and references therein). Drill monitoring is based on the conception of the relationship between drill parameters and rock characteristics. Drill monitoring has been extensively studied by many scientists (e.g. Honer and Sherrell 1977, Howard et al. 1986, Schunnesson 1997), but is still not a standard technique in the rock industry. The essence of drill monitoring is to explore the in situ rock characteristics of a rock mass, and extract useful information from automatically collected borehole data.

The drillability of rocks are mainly dependent upon operational variables and rock characteristics (Kahraman et al. 2003). Operational variables are all parameters that can be controlled by an operator, such as rotation speed, thrust, blow frequency and flushing. Rabia (1985) concluded that the drilling strength is expected to correlate well to the compressive and impact strength of the rock. The drilling strength or drillability is a measure of how far the drill bit can penetrate the rock in a given time period.

In most modern drill rigs, microprocessor units, which ensures high penetration rate, controls operational variables automatically and ensures low bit wear throughout the borehole, however raw data are always disturbed by the influence of the operator, who adjusts the drill settings to achieve the best drilling result (Schunnesson 1997).

Schunnesson (1998) states that there is a great potential in using drill monitoring data from percussive drilling to characterize rock, because of the inexpensive and frequent technique used in both mining and construction industries. He also states that the raw data are collected in digital form, and is therefore fast to interpret on an ordinary computer and could also be an integrated part in the decision process in for example a tunnel operation.

Throughout the years, many automated drill monitor systems have been developed. A system called ADM (Automated Drill Monitor), developed by Solroc Inc. Montreal (Scoble et al. 1989) records and process drill parameters so that a precise definition of zones of changing

rock properties at depth in a borehole can be found. The ADM system can be mounted on any kind of drill rig, both percussion and rotary. Yue, Lee et al. (2003) developed a drill process monitor (DPM) that also can be integrated on every type of drill rig. It can automatically, objectively and continuously measure and record drilling parameters in real time, but it does not include a processing unit that can interpret and visualize rock characteristics from the drilling parameters. Atlas Copco has developed a program, Tunnel Manager MWD, which follows the IREDES standard. Tunnel Manager MWD can interpret drill parameters collected from drill rigs, and display 3-dimensional calculations of all drill parameters and also rock hardness and fracturing.

### **2.3.2 Drill parameters**

When rotary percussive drilling in rock, the parameters collected are essential for interpreting the in situ rock conditions through drill monitoring. Various parameters can be collected and calculated, but during drilling, according to Schunnesson (1997), the most important and most regularly collected parameters are:

- Time at which data is sampled (h-m-s)
- Drill hole depth (distance)
- Penetration rate (distance/time)
- Thrust (feed pressure)(bar or kN)
- Torque pressure (bar)
- Percussive pressure (bar)
- Rotation speed (RPM)

Additionally there are more parameters that can be collected from the drill rig:

- Water pressure (bar)
- Water flow (liters/minute)

The files generated by the drill rigs are usually in the form \*.MWD. MWD is an abbreviation for Measurement While Drilling, and the term originates from the oil industry.

The parameters can be divided into two groups: One group for dependent parameters and one group for independent parameters. The independent parameters, also called operational

variables, are parameters that can be directly controlled by the operator, such as e.g. feed thrust, rotation pressure and percussion pressure. The dependent parameters however, are dependent both upon the other parameters and the geological features of the rock. The two most important parameters for rock characterization are the penetration rate and the torque pressure (Schunnesson 1998), which are both dependent parameters. The normalized penetration rate is a good indicator for rock hardness and torque pressure for fracturing. The torque pressure is dependent on hole-length, as the friction between the drill rod and the rock wall inside the borehole increases as the borehole length increases. Also the torque pressure is dependent on the penetration rate, and therefore it is hard to separate hole length dependent torque from penetration rate dependent torque.

In their work, Howarth and Rowlands (1987), Thuro (1997) and Kaharaman et al. (2003) have done research on drillability, and found several geological parameters that influence the penetration rate. Thuro (1997) mentions four of the most important: anisotropy – the orientation of discontinuities related to the direction of testing and drilling, the spacing of discontinuities, the mineral composition, and the pore volume.

Different test methods, as the Brazilian tensile strength and Schmidt hammer value have shown strong correlation with penetration rate (Kahraman et al. 2003). Unconfined compressive strength is the most frequently used strength test for rocks, but it still has its disadvantages; it is not simple to perform properly and results can vary by a factor of more than two as procedures are varied (Goodman 1989). Tsoutrelis (1969) found that the rate of penetration from a hard metal drill bit, correlates with the compressive strength of the rock, however it should be mentioned that this test was done only by rotational drilling. Kahraman et al (2003) also conducted drillability tests that confirmed that the uniaxial compressive strength and penetration rate was well correlated. They also confirmed that the point load index correlate to the penetration rate. The above confirm the statement that the penetration rate and torque increase when rock hardness decrease (Sinkala 1991).

## 2.4 Tunnel Manager MWD

Tunnel Manager MWD is a program developed by Atlas Copco AB. It is a tool for planning, administration and evaluation of drill parameters and drilling operation in tunnel and mining industry. From collected MWD files, holes can be viewed in 3D, single parameters can be shown as graphs and mapping of tunnel line can be calculated for both hardness and fracturing.

Tunnel Manager MWD is built for Microsoft Windows and can generate reports in .doc formats. It is in general a helpful tool for the planning process, and especially the calculated hardness and fracturing tool can be valuable to production planning and safety measures.

The hardness and fracturing algorithm is based upon the theory of Schunnesson (1996, 1998), and does supposedly show good correlation with uniaxial compressive strength and RQD. The software can be modified for calibration of rock hardness and fracturing along with site-specific normalization with C++ programming language.

Tunnel Manager MWD is not a substitute for engineering geological mapping, but is a supplement tool for assessing more information during excavation and planning.

## 2.5 Normalization of borehole parameters

When drilling in hard rock, as stated in section 2.3, various responses can be recorded: the properties of the rock itself, variations caused by the changes in rock condition, and other variations caused by the drill rig itself (Schunnesson 1998). Every drilling machine has its own “signature”, a typical variation or pattern in borehole parameters, that has to be removed from the raw data before an analysis can be done. During tunnel construction with the drill and blast method, large amounts of drill parameter data are recorded, and by using averages, based on these data, unsystematic variation caused by variations in rock conditions is evened out, while the systematic variation from the drill rig itself remains (Schunnesson 1998). The systematic variations are mostly dependent on the borehole length. This pattern from the drill

rig then has to be identified, so that it can be removed from every dataset/hole. Then the analysis will only be based on drill data variation caused by variations in the mechanical properties of the rock.

There are different paths to detect the systematic variations caused by the rig. Most drill parameters are dependent on each other as described in section 2.3.2, meaning for example that the torque is both dependent on the penetration rate, feed thrust and the borehole length.

To normalize the data for borehole length dependent variation, Schunnesson (1998) suggest a quite straight forward step by step method. All borehole data are collected, averaged and plotted. A regression line is calculated, and the gradient of the regression line is then the basis that the normalization for borehole length is built on. In other words, the gradient of the trend line is withdrawn from every dataset. In this way all drilling is assumed at zero depth. To ensure that the process of normalization is good enough for detecting variations in rock conditions, there has to be a sufficiently large amount of drill response data, so that the variations caused by the drill system remains, and can be withdrawn. Following the normalization of variations for borehole depth, normalization of penetration rate and torque pressure for feed pressure dependent variation are conducted, and finally by removing the influence of penetration rate on the torque pressure.

The regression line for penetration rate would in general show a declining trend over borehole depth. This declining trend is a combination of numerous reasons. Schunnesson (1998) describes some of the most significant factors that affect the penetration rate for top-hammer drills:

- The drill string joints in top hammer drills will absorb some of the incident stress wave energy.
- The flushing efficiency decreases as the borehole length increases.
- Bit wear

The borehole length, or whether the hole is drilled upwards or downwards also affects the variation of feed thrust. When increasing number of drill rods, the weight of the entire system increases, and a following a change of feed thrust, required to compensate for the gravitational force can be seen (Schunnesson 1998).

However as the penetration rate usually show a declining trend, the torque pressure, which is dependent on the feed thrust and the penetration rate, can show either an inclining or declining trend depending on the rock conditions and borehole length. The reason for this, is according to Schunnesson (1998) two contradictory phenomena: Due to the reduction in penetration rate with increasing borehole length, the torque required to rotate the bit will decrease, but on the other hand the torque will also increase because of the increased friction between the drill rods and the walls of the hole. Furthermore the variation of torque is also due to the increase or decrease of feed.

## 2.6 Rock Quality Designation and the Q-method

The Q-method is a system for classifying the stability of rock masses in tunnels and caverns.

The Q-method is based on six parameters and the Q-value can be calculated for any rock mass (Løset et al. 1997). Q-value range from 0.001 for exceptionally poor rock and up to 1000 for exceptionally good rock. The Q-value obtained, is related to different types and level of permanent support.

### Equation 2.1

$$Q = \frac{RQD}{J_n} \times \frac{J_r}{J_a} \times \frac{J_w}{SRF}$$

The six parameters used in the Q-method are:

- RQD – Rock Quality Designation
- $J_n$  – Joint set number
- $J_r$  - Joint roughness number
- $J_a$  – Joint alteration number
- $J_w$  – Joint water reduction factor
- SRF – Stress reduction factor

These parameters can be obtained through geological field mapping, mapping in tunnels and mapping of drill cores. There have been discussions regarding the accuracy of using RQD numbers in the Q system (Palmstrom and Broch 2006). The RQD is measured from drill core

samples, and can therefore, if main joint direction is parallel or near parallel to the drill direction, give RQD values that not are in correlation with the true rock characteristics. Palmstrom and Broch (2006) suggest therefore applying RQD with great care.

## 2.7 RQD Prediction in drill monitoring

At Glødberget, a railway tunnel in Sweden, RQD predictions has been made by Schunnesson (1996) upon collected drill parameters. RQD values are usually mapped only each 5 to 15 meters, and therefore the drill parameters has to be averaged over the same section as the RQD mapping to achieve correct values. The RQD prediction was based upon penetration rate, penetration rate variation, torque pressure, torque pressure variation, and in addition, the absolute value of each parameter.

### 3. Methodology and datasets

#### 3.1 Drill data in the Løren tunnel

The drill data and the engineering geological mapping has been collected by automatic drill rigs or engineering geologist at the site. The mechanical rock properties in Table 3.1 are collected by Haug et al (2007) from four drill core samples. The collected engineering geologic mapping data used in this thesis range from chainage 1300 to chainage 1500 in tunnel-line A and from chainage 1280 to chainage 1540 in tunnel-line B and can be found in Appendix. The MWD data range is from chainage 1300 to chainage 1531 in A and chainage 1285 to chainage 1521 in B.

The excavation of the tunnel started from Northwest, and thus the drill direction is from high to low chainage numbers.

**Table 3.1 The mechanical properties of different rock types found in drill cores in the Løren tunnel. (modified from Haug et al. 2007)**

From meter	To meter	Rock type	Point Load test Is50 Mpa	Unconfined compression Mpa	Rock Strength ISRM 1978
116	116	Syenite	8,9	178	Very High
162	163,5	Nodular limestone	3,2	45	Medium
187	187	Porphyry syenite	9	189	Very High
240	244	Black shale, breccia	2,9	41	Medium
261	266	Black shale	2,1	29	Medium
267	273	Shale	2,6	36	Medium

As the rock types in the Løren tunnel area, consists of sedimentary rocks with intruding igneous dykes, the boundaries between the two main rock types are quite obvious both visually and mechanically. Scoble et al. (1989) stated that monitored drilling techniques are most successfully implemented in geological areas where there is a defined contrast between rock types in terms of strength and lithology. According to their statement, the geological

boundaries in the Løren tunnel should be fairly easy to interpret cause of the natural boundaries between the igneous intrusive and the sedimentary rocks. As seen in Table 3.1 the mechanical properties between the two main rock types (sedimentary and igneous) differ considerably in terms of rock strength. The boundaries between the different sedimentary rocks, are not that big, and the boundaries between those, might be harder to detect from the drill monitoring data.

## 3.2 Drill equipment in the Løren tunnel

Atlas Copco AB supplies the drill equipment in the Løren tunnel. The drill rig is of the type Boomer XE3 that has three booms with the COP 3038 rock drill.

The COP 3038 is a 30kW hydraulic rock drill developed for face drilling in the tunnel industry. The borehole diameter range is from 43 to 64 mm, and the maximum drilling rate is about seven meters per minute.

## 3.3 Visual verification of Tunnel Manager models

Tunnel Manager MWD has the ability to produce models of all included drill parameters and also models of rock hardness and fracturing. The calculated parameters rock hardness and fracturing in Tunnel Manager MWD, are not site specific calibrated, but instead calibrated by using data gathered from many projects.

To map geological features over tunnel length, two datasets are needed. First the MWD data files which contains the drill parameter values, and second the tunnel line coordinates so that the MWD data are placed at the right position.

The models are draped over a theoretical tunnel line and some distortion between the excavated tunnel and the theoretical may exist. Also the calculated models, or mapped tunnel lines, does rely on correct settings. The settings adjust the dimensions of the tunnel, as height and radius, but also adjust the level of influence each borehole has on the next nearby hole.

The settings also include options to set plane thickness, which is the thickness of the projected plane.

In order to get a good visualization of the wanted features it is important to set the color scaling to the right intervals. One can choose both the interval and the color of choice. If these settings are not adjusted correctly, one could easily miss important geological features, especially in hardness. E.g. the shale and the syenite, where the latest has a UCS almost five-folded the shale, could be interpreted as same rock if color scaling is incorrectly set. In general, the visual verification of the Tunnel Manager constructed models is highly dependent upon the color-scaling interval.

Since the software is not calibrated for any specific type of rock, one interval of hardness or color may include many different types of rock.

### 3.4 Program for calculated average

As the borehole data consist of thousands of data files, and therefore would be very time consuming if averages were to be calculated by hand, a program has been written to manage the large datasets. The programming language is Python, which is a free open source language, and it can be run on Windows, OS X and Unix/Linux. The term “reading number” (RN) is used throughout the thesis and is a dimensionless value connected to the sampling frequency of the data.

The way the program works is pretty simple and can be summarized as following:

1. The program itself is placed in the folder where the raw data is situated, and is launched
2. It gathers all of the variables in the desired column (the desired column can be changed by modifying the script)
3. It generates an average of all the variables chosen
4. Finally, the averages are written to a text file along with the number of calculations used in each reading to calculate the average.

The program does not calculate the average for every borehole length, instead it use the number of the reading. This means that it can be somewhat sensitive if there is not enough data, but in usual, the readings are so close that in a long run, and with a sufficient amount of data this will be averaged out. As there are two columns of data, the first is the averaged data and the second is the number of data ( $n$ ) the averages are based on. The entire program can be found in *Appendix II*.

### 3.5 Normalization process for borehole depth

As mentioned in section 2.3.2 the borehole depth affects the dependent parameters. To remove this variation from the dependent parameters a trend calculated from the averaged data is used. The trend represents the variation over borehole depth.

The average of the collected drill data are sorted regarding borehole type: injection-holes or blast-holes. The Python program is then set for the desired parameter to be averaged.

The result of the calculation are then plotted and inspected visually.

In order to get a representative regression line, data from the beginning of the hole will most likely have to be removed. When the selection of data is chosen, a regression line can be calculated. The difference between the regression line and the regression line's average is the variation to be removed (Figure 3.1).

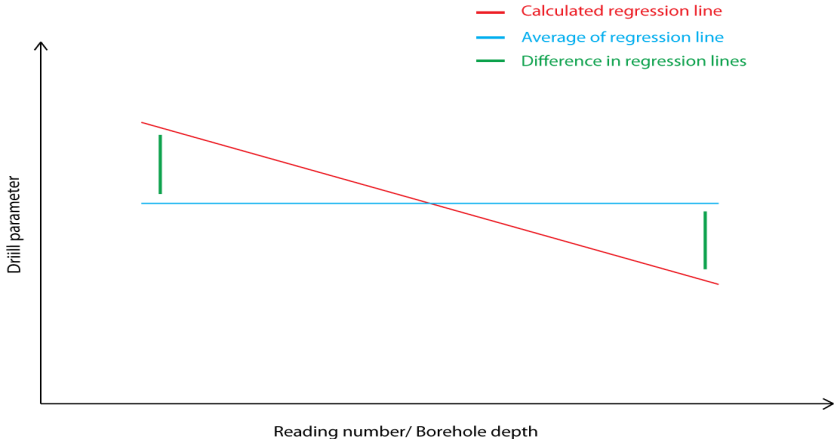


**Figure 3.1. Demonstration of how the regression line is modified for borehole depth**

### 3.6 Normalization process for feed thrust

During drilling the feed thrust ensures that the drill bit is in contact with the bottom of the borehole so that a forward motion, or a rate of penetration, is generated. Following this, the penetration rate and torque pressure will be highly dependent upon this parameter. The way to remove the variation of feed thrust on penetration rate and torque pressure is proceeded in the same way as the depth normalization, but instead of plotting against borehole depth, the penetration rate and torque pressure are plotted against feed. It is although important to remember that all the parameters have to be normalized for depth variation before normalization for feed thrust is done.

### 3.7 Normalization process for penetration rate dependent torque and torque dependent penetration rate

As mentioned in section 2.3.2, the penetration rate is dependent upon the torque and vice versa. In order to use the torque pressure as a parameter for rock characterization, the variations caused by the penetration rate has to be removed. However this relation is usually not linear as the torque pressure can be high at low penetration levels, and at high penetration rates where the torque pressure show a decrease (Schunnesson 1998, Liu and Yin 2001). To normalize the torque pressure for penetration rate, the data has to be plotted and a regression line chosen from the parts of the plot where there are linearity between the two parameters. The same procedure has to be done to the penetration rate (removal of the effect of torque pressure).

Both the torque pressure and the penetration rate have to be normalized for both borehole depth and feed thrust in order to perform this normalization.

### 3.8 Inspection of normalized parameters

The inspection of normalized borehole parameters will be done by visual comparing of these to the hardness and fracturing mapping in Tunnel Manager and the engineering geological mapping. Changes in trends, variability and identification of peaks will be the main factors to be looked for. Zones with both good and bad correlation will be subjected to analysis so that eventual weakness of the normalizing process can be identified.

### 3.9 Test of rock hardness vs penetration rate

As earlier test of the relationship between UCS and penetration rate has been conducted and correlation has been concluded (Kahraman et al. 2003), an investigation of the rock types and penetration rate in the tunnel will be emphasized. The python program will be used to generate averages of the penetration rate on selected rocks, and the averages will be compared to the UCS (Table 3.1) collected by the preliminary studies conducted by Haug et al. (2007).

The selected rocks are: shale, nodular limestone and syenite. The reason for selecting these three rock types are because they are abundant and the thickness of the rock structures can be larger than the average blast hole drill length. It is predicted that the syenite will show the lowest average penetration rate as it has the highest UCS and the two sedimentary rocks will be much closer in terms of penetration rate.

Because of the changing geology in the tunnel, injection holes will in most cases intersect more than one rock type, and thus will not be used for generating penetration rate averages that can be related to UCS.

It is used raw data in this analysis, because an average of entire datasets are calculated and normalization would not alter the data to a certain degree as the normalization is based upon variances from the average value of the regression line.

The chosen penetration rate data consist of following:

Syenite: chainage A1360 to A1370 and chainage B1375 to B1385

Nodular limestone: chainage A1375 to A1385 and chainage B1410 to B1430

Shale: chainage A1445 to A1470, chainage A1505 to A1540, chainage B1450 to B1465 and chainage B1480 to B1510

The drill data used in the process range from reading number 50 to 200. This process will be not as sensitive towards trends as the normalization process for dependent parameters, as the average values are used.

## 4. Results

### 4.1 The normalization process

#### 4.1.1 Normalization for borehole depth

As described in section 3.5 the normalization process is based upon the regression lines calculated from the data obtained from the python program (*Appendix II*). Following Schunnessons (1998) paper “Rock characterization using percussive drilling”, the parameters undergoing normalization are penetration rate, torque pressure and feed thrust.

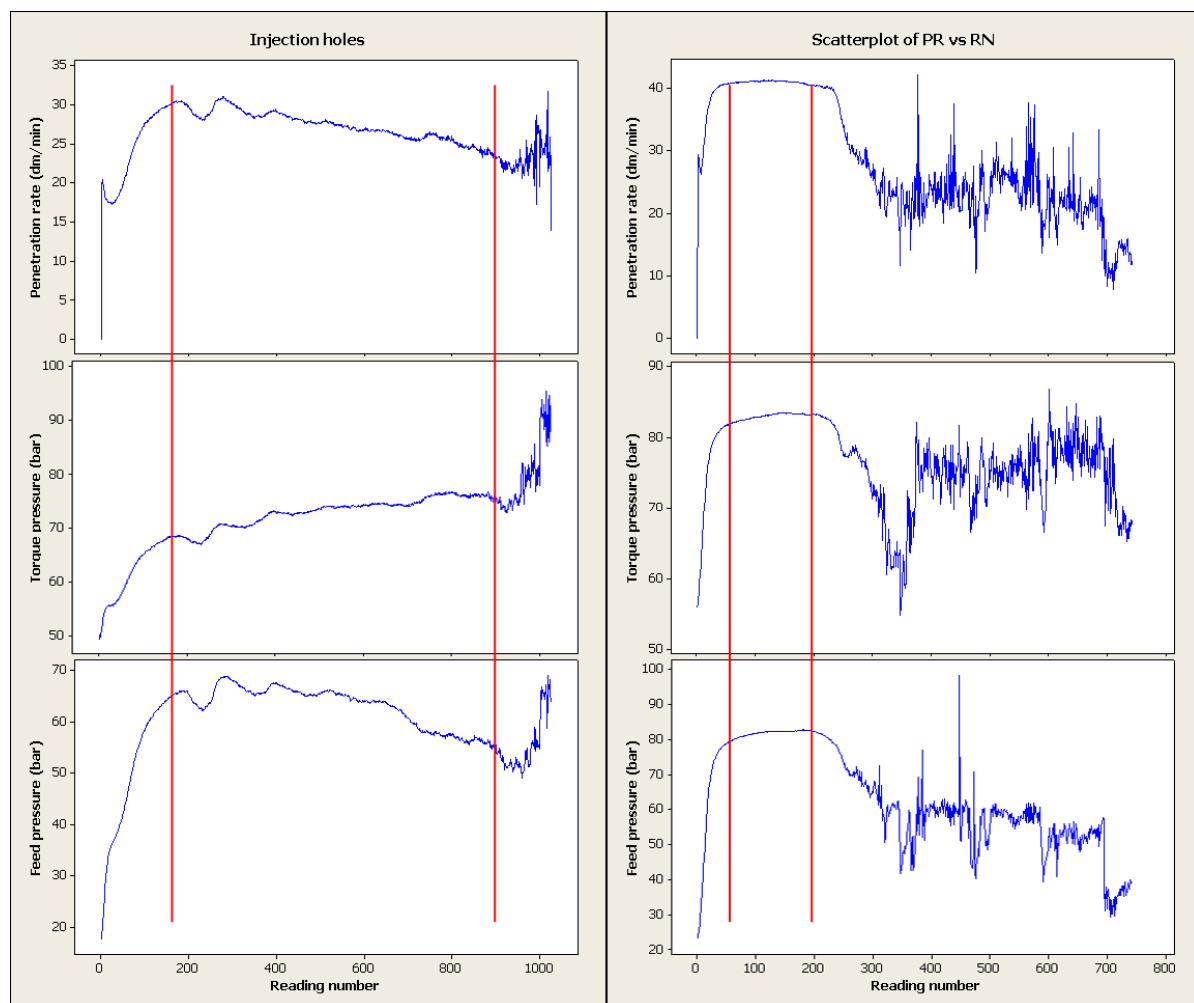


Figure 4.1. Calculated averages from injection holes (left), and blast holes (right). Data outside the red lines are ignored in the regression calculation.

In Figure 4.1 penetration rate, torque pressure and feed thrust averages are plotted for injection and blast holes. It is the values between the red lines that the regression is calculated upon. Two thresholds are chosen for each parameter and borehole type. The low threshold is based upon where the graphs flatten out which represents the average reading number where the drill hammer has reached the maximum value, and the high threshold is based upon the reading number where the number of calculated averages decrease rapidly or scattering of average is seen in plots. For injection holes this threshold is located at reading number 883 where the number of averages drop below 300. For blast holes the threshold is located at reading number 194 where the thrust and torque pressure plots start to decline.

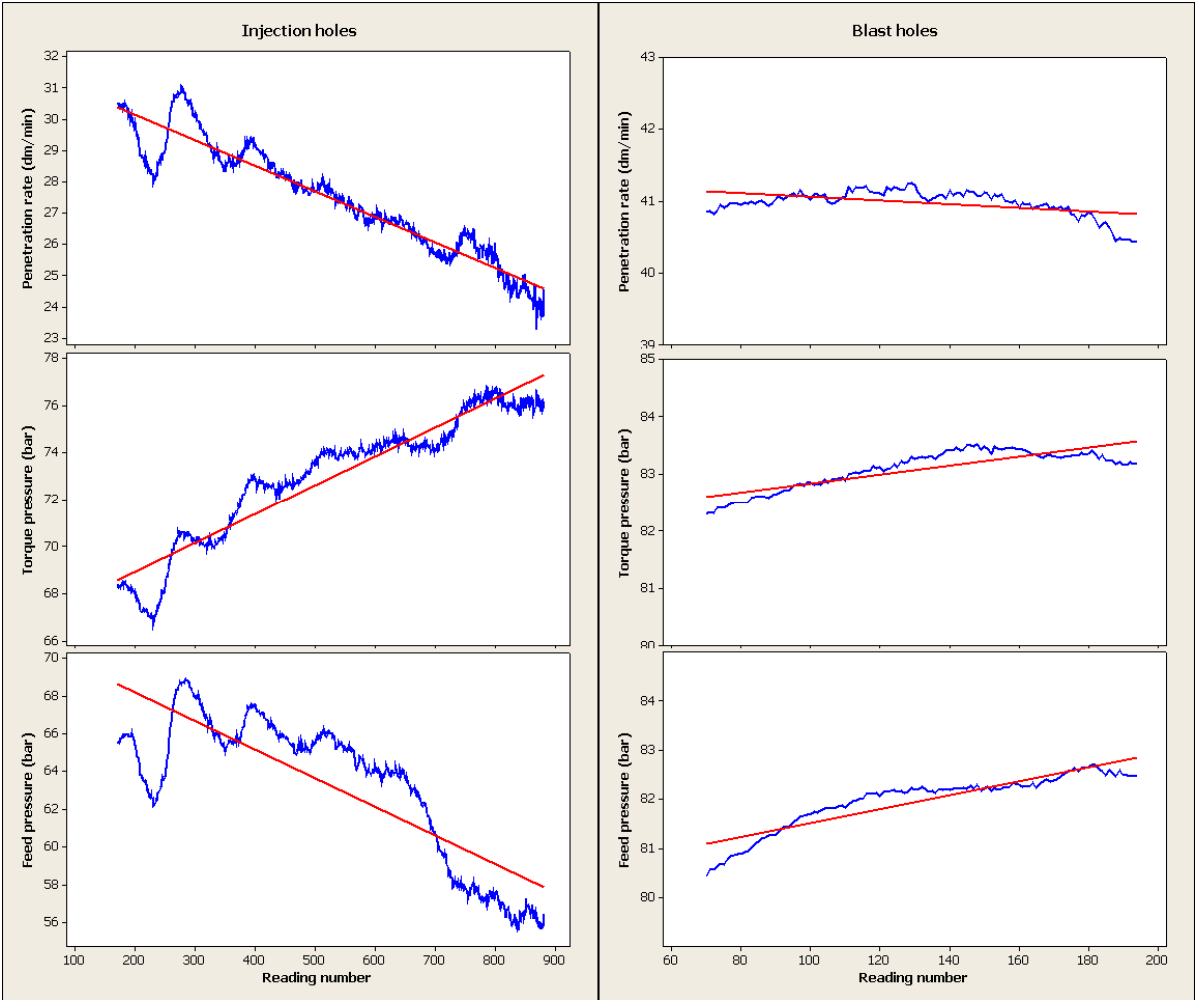


Figure 4.2. Modified averages with regression.

In Figure 4.2 the modified averages are plotted with regression line. The regression line for penetration rates from both borehole types show a negative trend over borehole depth.

The two torque pressure plots show both positive trends. The feed thrust plot for injection holes show a negative trend, while the feed thrust for blast hole show a negative trend. The

regression lines are calculated by least squares regression, so that the squared distance between the data points and the line is minimized.

**Table 4.1. Equations for regression lines in Figure 4.2.**

<b>PR regression injection</b>	<b><math>PR_{inj} = 31,81 - 0,008204 * RN</math></b>
<b>TP regression injection</b>	<b><math>TP_{inj} = 66,48 + 0,01230 * RN</math></b>
<b>FP regression injection</b>	<b><math>FP_{inj} = 71,19 - 0,01512 * RN</math></b>
<b>PR regression blast</b>	<b><math>PR_{blast} = 41,32 - 0,002609 * RN</math></b>
<b>TP regression blast</b>	<b><math>TP_{blast} = 82,04 + 0,007884 * RN</math></b>
<b>FP regression blast</b>	<b><math>FP_{blast} = 80,10 + 0,01414 * RN</math></b>

The data presented in Table 4.1 is the equations for the regression lines in Figure 4.2. RN is an abbreviation for reading number, PR for penetration rate, TP for torque pressure and FP for feed pressure (feed thrust).

The regression line is subtracted from the respective datasets by finding the difference between the regression line and the average value of the regression line. This difference is then subtracted from the dataset. The result is parameters normalized for borehole depth, and the calculations can be found in *Appendix II*.

### 4.1.2 Normalization for feed thrust

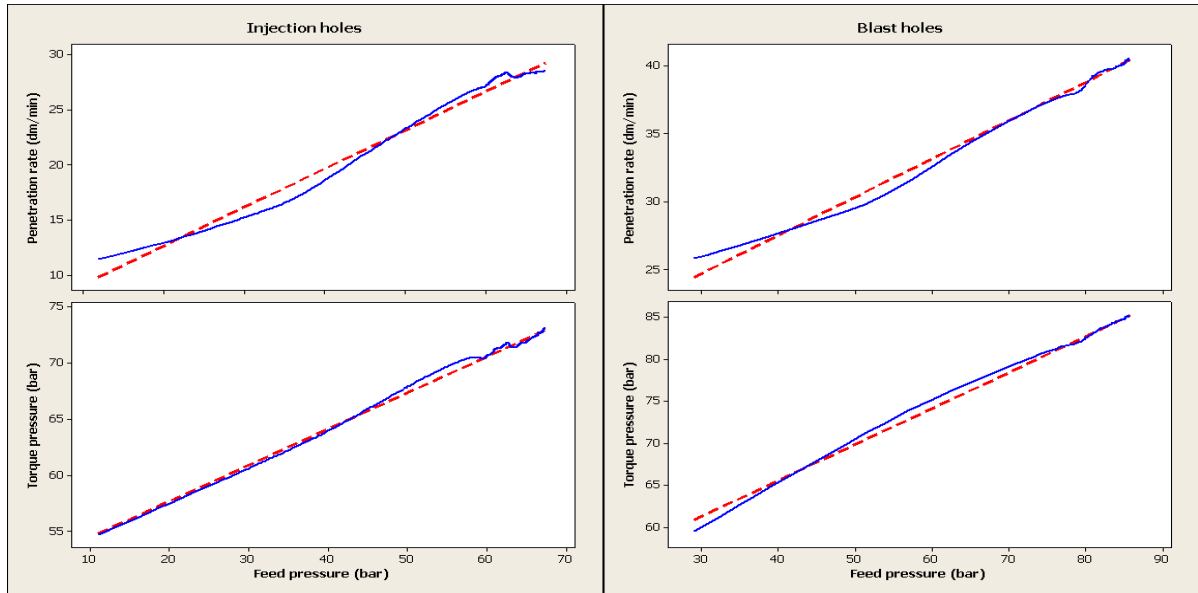


**Figure 4.3.** Averaged penetration rate and torque pressure plotted against feed thrust for injection holes (left) and blast holes (right). The parameters are normalized for borehole length. Blue lines are locally weighted scatterplot smoothing (LOWESS) fit for the averaged data, and the red dotted lines the linear regression lines.

In Figure 4.3 the penetration rate and torque pressure from injection holes are plotted against feed thrust. The plots are presented as LOWESS to easier get an understanding of the correlation between the parameters. All plots show an increase in penetration rate and torque pressure for increasing feed thrust.

**Table 4.2** Equations for regression lines in Figure 4.3.

PR regression injection	$PR_{inj} = 5,714 + 0,3485*FP$
TP regression injection	$TP_{inj} = 51,23 + 0,3217*FP$
PR regression blast	$PR_{blast} = 16,27 + 0,2816*FP$
TP regression blast	$TP_{blast} = 48,41 + 0,4288*FP$

The normalization of penetration rate and torque pressure for feed thrust is based upon equations in Table 4.2. The normalization is done in the same procedure as for borehole depth normalization. The calculations can be found in *Appendix II*.

### 4.1.3 Normalization of torque and penetration rate

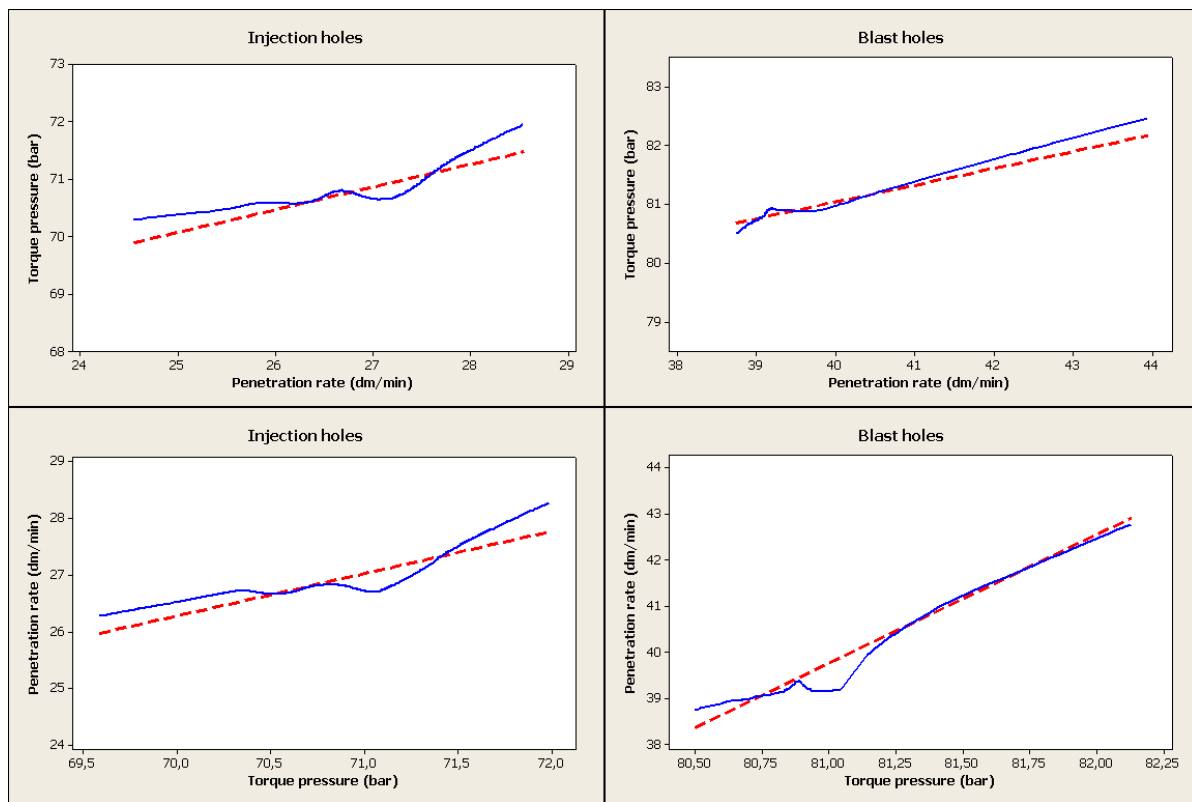


Figure 4.4. Regression lines for torque pressure and penetration rate. All parameters are normalized for borehole depth variation and feed thrust variation. Left side injection holes, right side blast holes. The blue line represent a LOWESS fit of the data and the red dotted lines represent the linear regression.

The plots in Figure 4.4 show the correlation between torque pressure and penetration rate. Both parameters are plotted against each other so that a regression line can be calculated for each dependent variable. In order to get a trend line representative for the dependency between the two parameters (chapter 3.7), penetration rate above 42,9 dm/min and torque pressure below 80,4 bar have been removed from the blast borehole data. In injection borehole data penetration rates above 28,5 dm/min have been removed.

Table 4.3. Equations for regression lines in Figure 4.4.

PR regression injection	$PR_{inj} = -25,97 + 0,7464*TP$
TP regression injection	$TP_{inj} = 60,18 + 0,3956*PR$
PR regression blast	$PR_{blast} = -186,2 + 2,790*TP$
TP regression blast	$TP_{blast} = 69,62 + 0,2855*PR$

The equations for the regression lines calculated from Figure 4.4 are shown in Table 4.3

#### 4.1.4 Sample of normalized borehole data

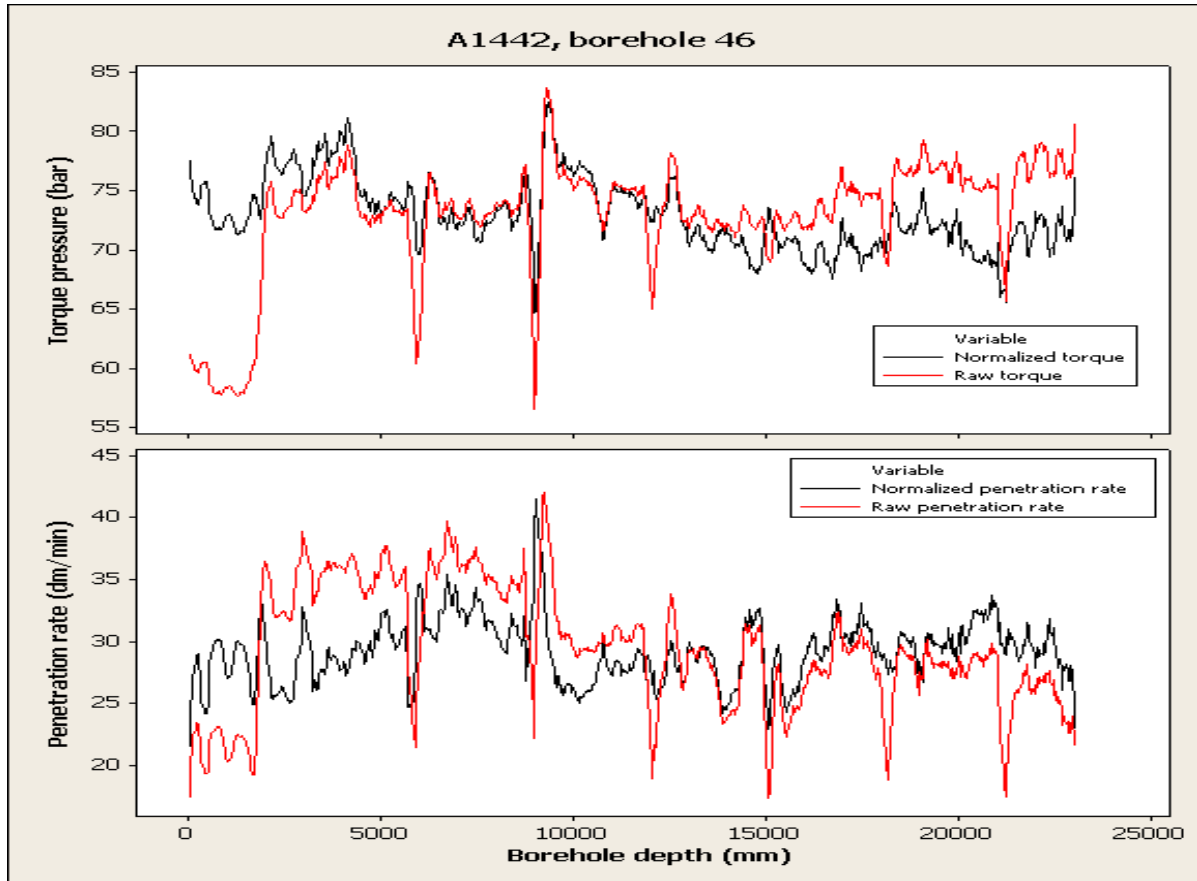


Figure 4.5. Raw and normalized torque pressure from chainage A1442 injection hole 46. The data are modified with floating average for easier comparison.

In Figure 4.5 the torque pressure and penetration rate are normalized for depth, feed thrust and penetration rate/torque pressure. At shallow borehole depths, the torque pressure is highly underestimated in the raw data. The central parts of the borehole are not that much affected, but at high borehole depths the raw torque pressure is fairly overestimated. After normalization the data has undergone a floating average modification to smoothen out the data. The floating average is based upon the eight following values.

## 4.2 Geomechanical interpretation

### 4.2.1 Chainage A1386

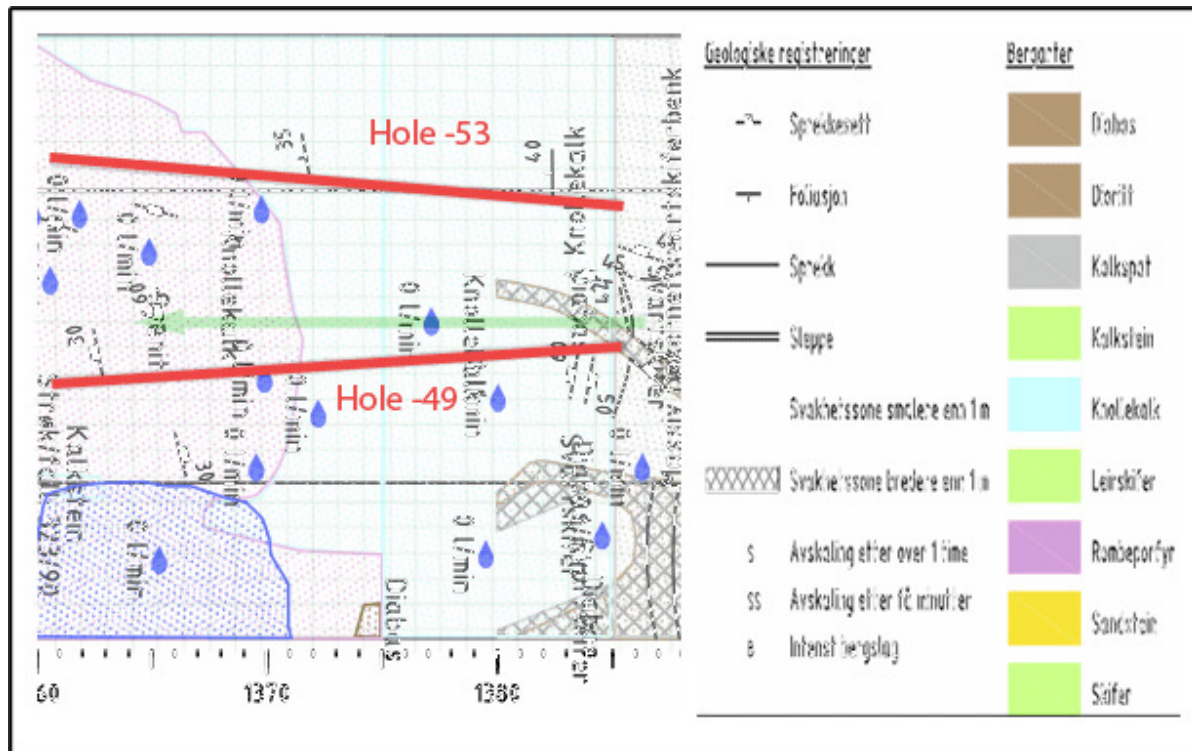
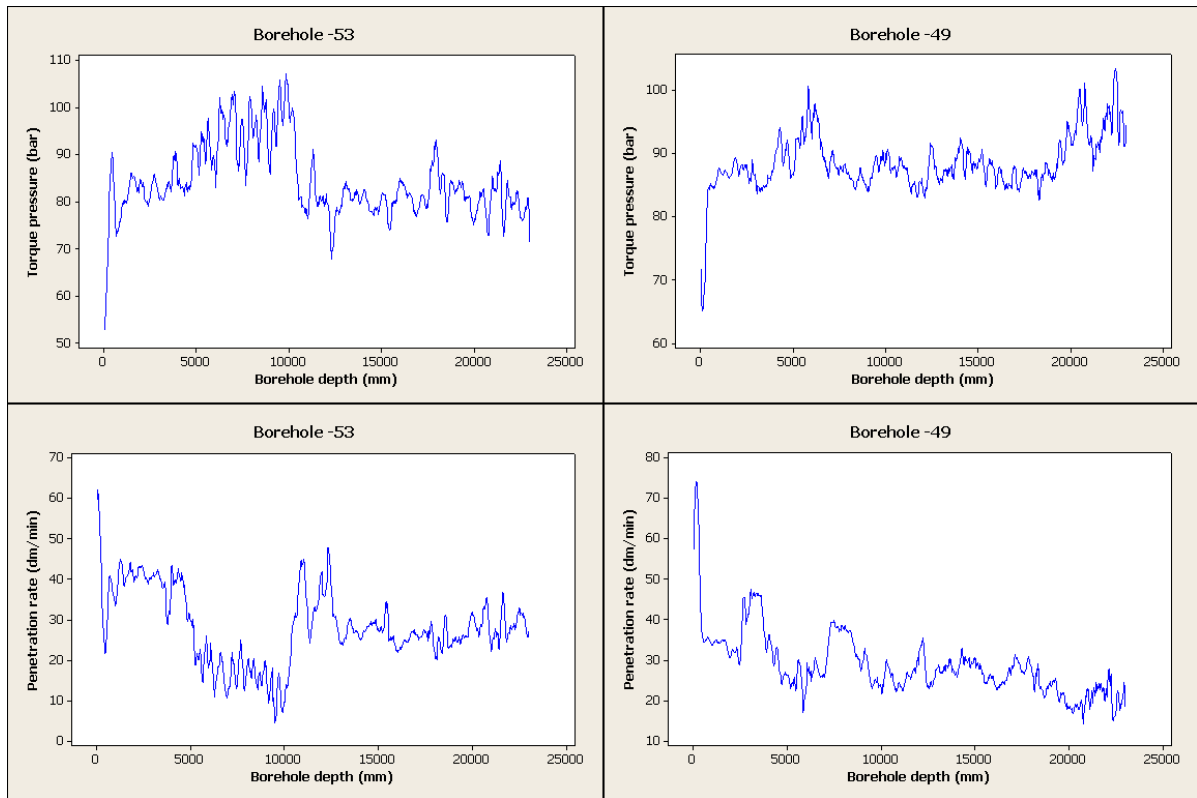


Figure 4.6. Location of boreholes -53 and -49. Section from chainage A1386

The injection boreholes in chainage A1386 starts out at a boundary between black-shale and nodular limestone. The limestone continues for about 14 meters before the syenite intrusive is seen. The shape of the syenite is not uniform over the tunnel chainage and the different boreholes will not reach the syenite at the same depth. Because of the shape of the syenite it is hard to tell the direction of it, and thus where the boreholes will intercept. One would predict lower penetration rates and torque pressures in the syenite versus the limestone.



**Figure 4.7. Normalized torque pressure and penetration rate for chainage A1386 holes -49 and -53**

In general the penetration rates from both boreholes show a decrease over borehole length in Figure 4.7. Borehole -53 has a marked shift in both penetration rate and torque pressure over the interval 5 to 10 meters depth. The parameters in borehole -49 show less variation than borehole -53 except from the first readings. At approximately 3 meters depth the penetration rate in borehole -49 peaks. In the same interval there is a slight reduction in torque pressure. After the peak in penetration rate a reduction can be seen. This reduction in penetration rate coincides with an increase in torque pressure. Further, both parameters show low variation until torque pressure rises at approximately 19 meters borehole depth. In this section the penetration rate slightly decrease.

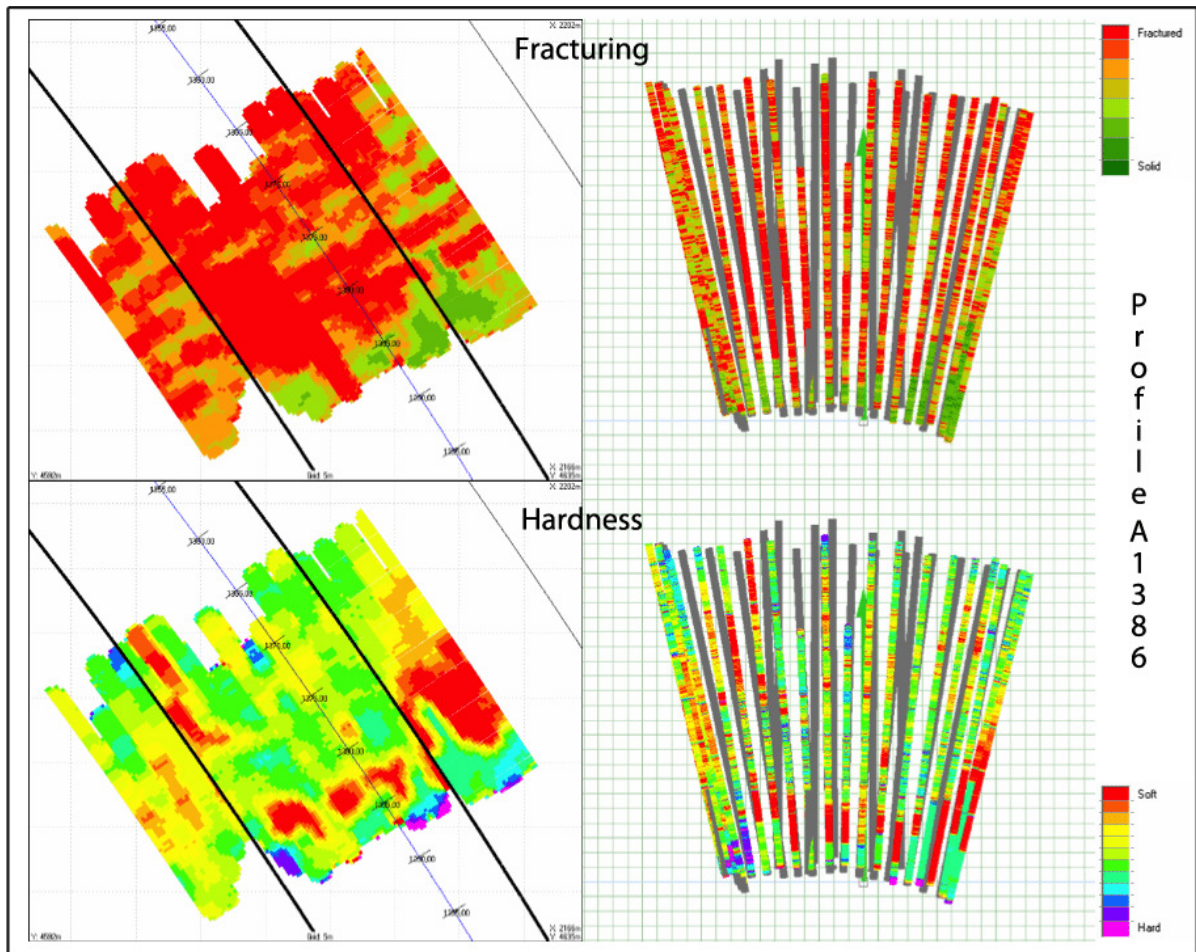


**Figure 4.8. Calculated fracturing and hardness mapping (left), and calculated fracturing and hardness in boreholes (right) from chainage A1386. All images and parameters generated by Tunnel Manager.**

In Figure 4.8 a zone of softer rock is mapped at the beginning of the chainage. This softer rock could be interpreted as the nodular limestone, but from the engineering geological mapping it is found that the rock type extend to almost 15 meters in thickness. This does not correlate well to the mapping done by Tunnel Manager. It is also hard to see the border between the syenite and the nodular limestone from the Tunnel Manager generated images. In general the level of fracturing is high in the entire section.

## 4.2.2 Chainage A1442

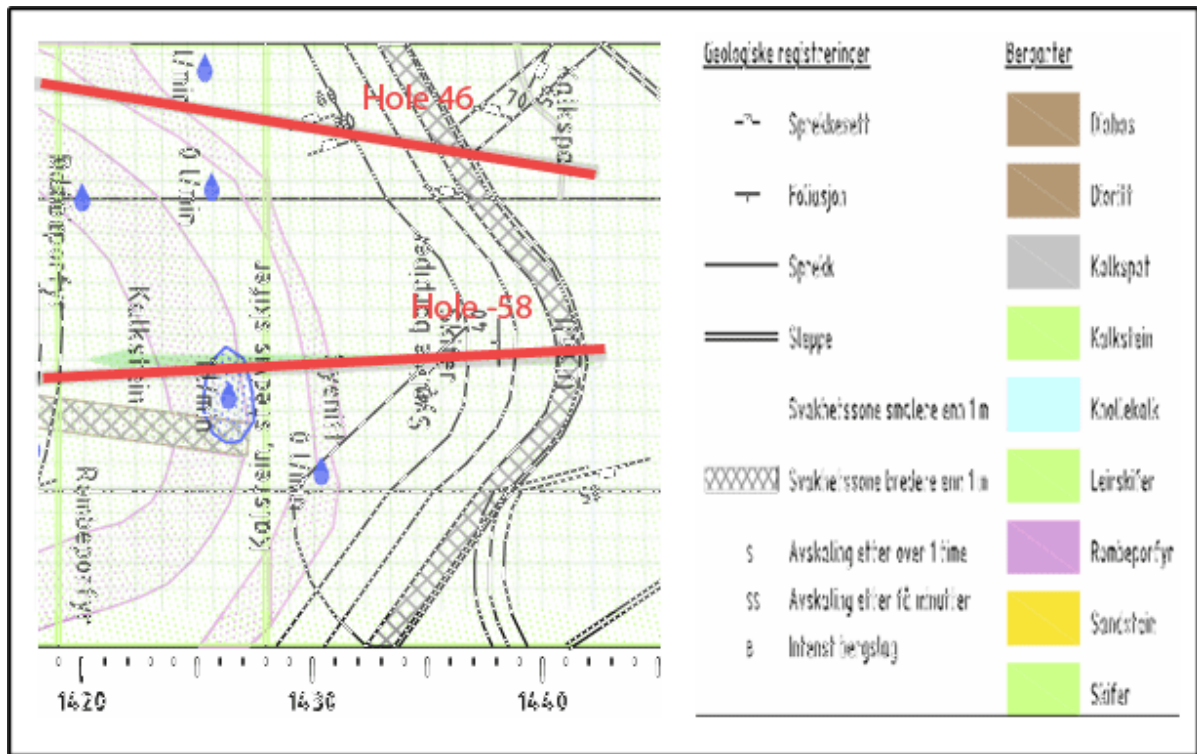
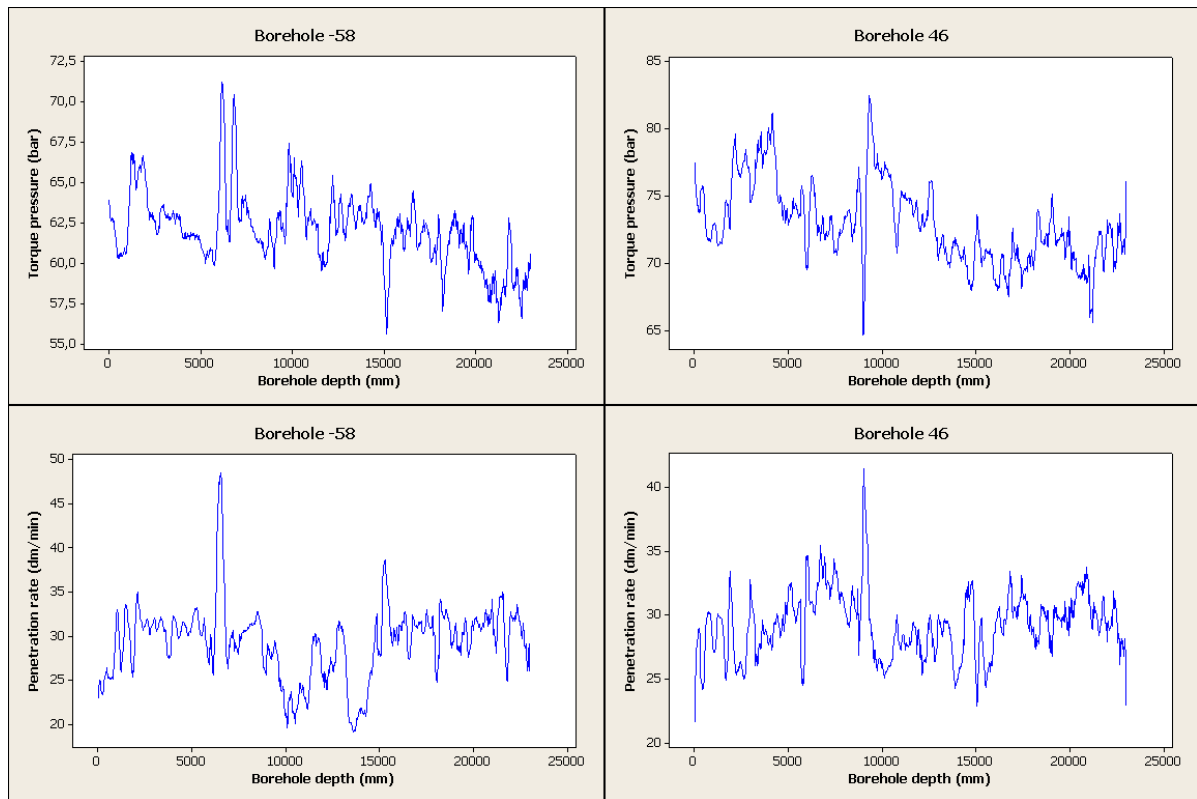


Figure 4.9. Location of boreholes 46 and -58. Section from chainage A1442.

In tunnel section from chainage A1442 the main rock type is shale and limestone. The borehole runs through a zone of weakness thicker than 1 meter and two syenite dykes with thickness of 2 to 4 meter.

In the zones of weakness one would expect an increase in torque pressure levels and variation in penetration rates, and where the drill bit crosses syenite dykes, a reduction in both penetration rate and torque pressure (Schunnesson 1998). Since the direction of the injection holes are tilted upwards, and the direction of the dykes and weakness zone are not vertical, the drill bits probably reached the zones somewhat earlier than seen in Figure 4.9.



**Figure 4.10. Normalized penetration rate and torque pressure for chainage A1442 holes 46 and -58**

In Figure 4.10 the two boreholes are plotted for torque pressure and penetration rate. In overall the penetration rates seem to be at pretty much same level, except for around depth 10 to 15 meters where the penetration rate decreases. The penetration rate for borehole -58 peaks around 7 meters depth. This peak might reflect the second fracture if looking in borehole direction. The peak registered around 9 meters hole depth for penetration rate hole 46 might also be one of these fractures. However it is hard to tell which of the fractures that are recorded. In the engineering geological mapping there are marked two fractures, but both penetration rates only show one peak in this interval. For the torque pressures, peaks are registered at the same locations as the penetration rates, but the torque pressure for borehole 46 also has a marked negative peak immediately before the positive peak.

At hole depth 10 to 15 meters, the penetration rate for hole -58 decreases over to intervals about two and three meters thick. In the same intervals the torque pressure also increases. The reduction in penetration rate and torque pressure values might indicate a zone of fracture. However there are not marked any fractures in this area.

In borehole 46, from borehole depth of about 10 meters to 15 meters, the penetration rate is generally lower than in other parts of the borehole.

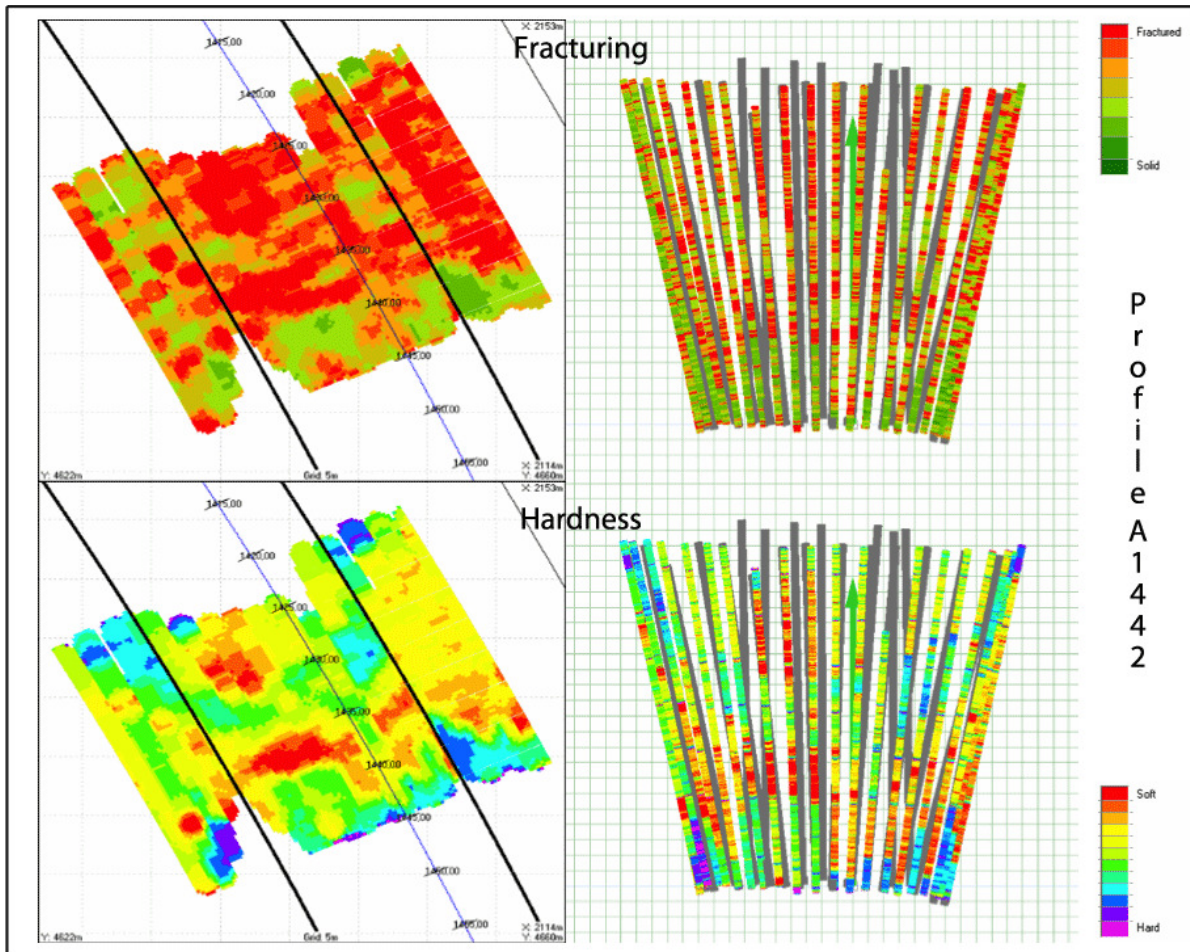


Figure 4.11. Calculated fracturing and hardness mapping (left), and calculated fracturing and hardness in boreholes (right) in chainage A1442. All images and parameters generated by Tunnel Manager.

From Figure 4.11 we can see the contours of the syenite dyke in both the holes and mapping for hardness. This is seen as a blue/green arched belt crossing the section. However the fracture zone is not reflected in the fracturing mapping or fracturing holes, but instead the softer parts discovered by the hardness mapping may be a result of the fracture zone.

## 4.2.3 Chainage A1453

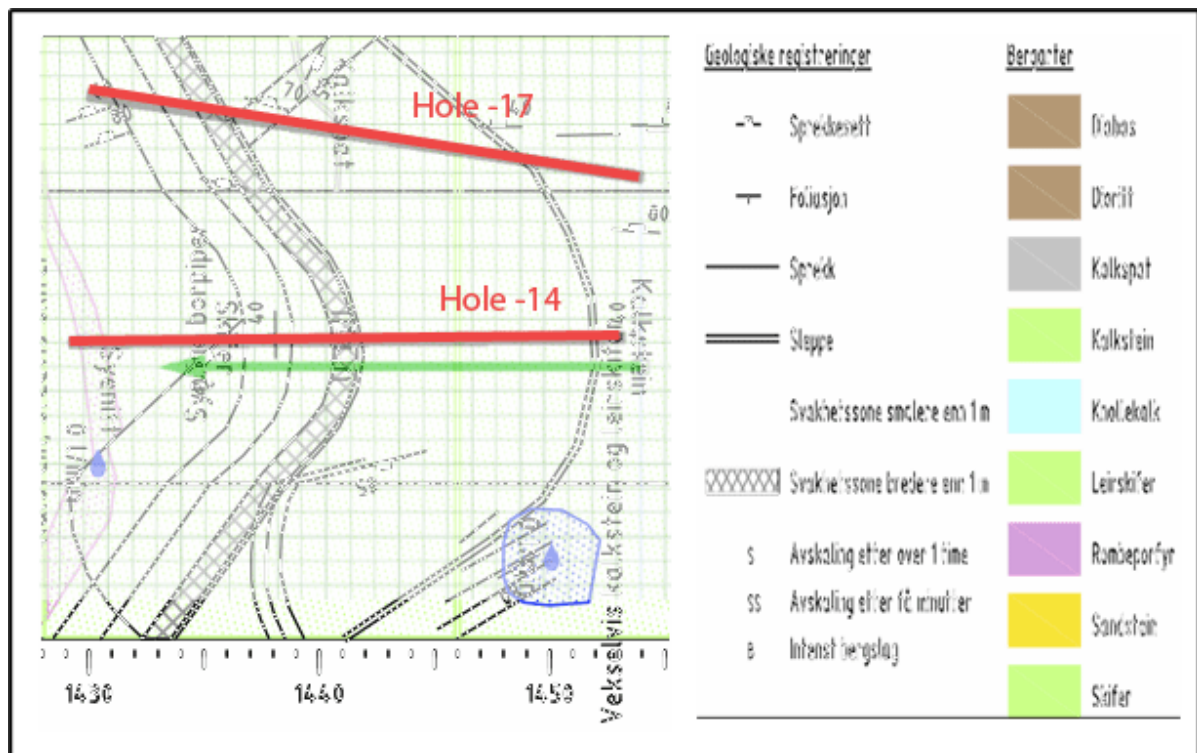
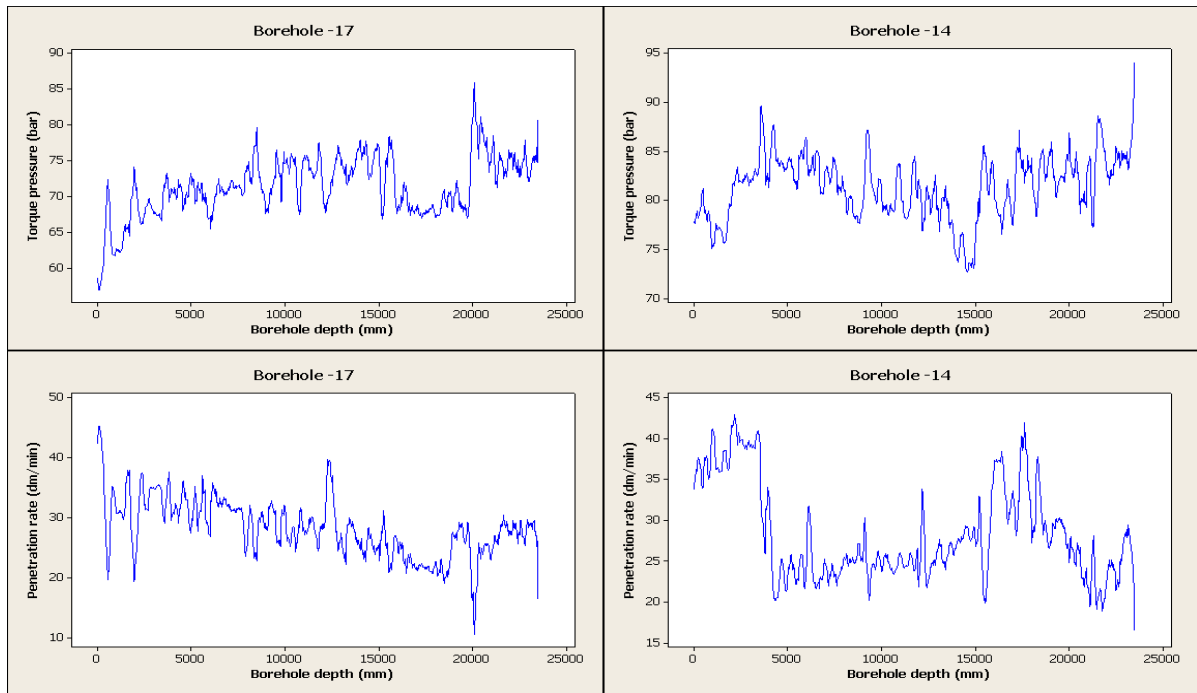


Figure 4.12. Location of boreholes -17 and -14. Section from chainage A1453.

Section number A1453 consists of the same rock types as section A1442 and will be expected to reflect some of the same structures. However there is a fracture zone located only a meter from drill start at the middle of the hanging wall. This zone might be hard to spot if the drilling still is in its start up procedure. The drill bits for both holes will reach the fracture zone and the fractures earlier than the intercept that is shown in Figure 4.12. There are also mapped a syenite dyke at the end of borehole -14 where changes in parameters would be expected.



**Figure 4.13. Normalized penetration rate and torque pressure from chainage A1453, holes -14 and -17**

In Figure 4.13 the penetration rate and torque pressure for hole -14 and -17 in chainage A1453 are plotted. The torque pressure in borehole -17 shows a general increasing trend over borehole depth, while the trend in borehole -14 is subtler. The penetration rates in borehole -17 show a decreasing trend with low variability over borehole length, while borehole -14 has larger variability.

The peak in penetration rate for borehole -17 at 12 meters borehole depth is followed up with a negative peak in torque pressure. Between approximately 16 and 18 meters borehole depth the torque pressure show low values. At approximately 18 to 19 meters borehole depth the penetration rate increase while the torque pressure decrease. The peak in torque pressure located at 20 meters borehole depth is followed up with a negative peak in penetration rate.

In borehole -14 at around 4 meters depth, the penetration rate decreases drastically. At the edge of this decrease a peak in torque pressure is seen. At 9 meters borehole depth, a peak in torque pressure and penetration rate can be seen. The penetration rate and torque pressure also has a peak around 12 meters borehole depth. Between 4 and 15 meters borehole depth the penetration rate shows a positive trend while the torque pressure show a decreasing trend. At 16 meters borehole depth a negative peak is recorded in penetration rate, at the same borehole depth a positive peak is recorded in torque pressure. From 18 meters borehole depth

penetration rate shows a decreasing trend for the rest of the borehole. Torque pressure in the interval show a slight increasing trend.

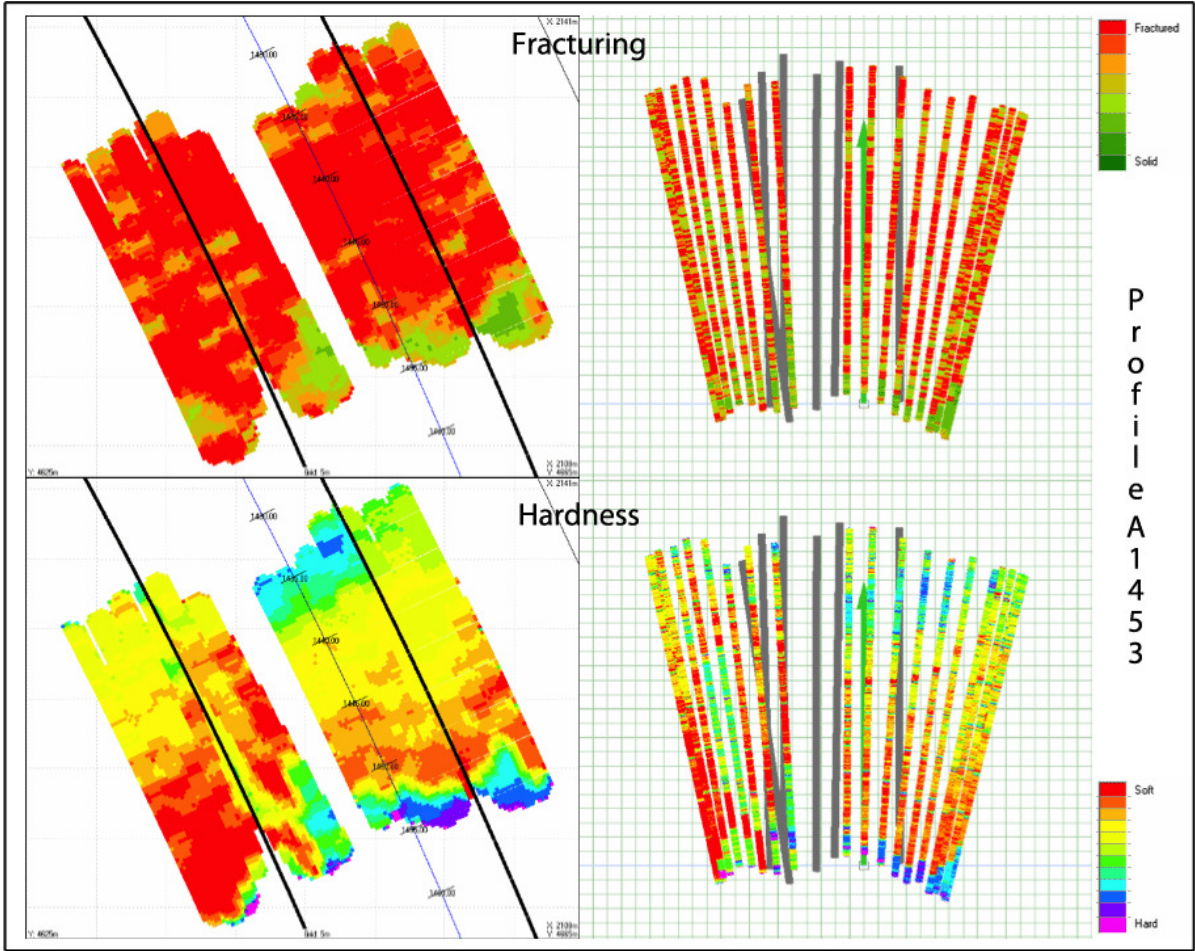


Figure 4.14. Calculated fracturing and hardness mapping (left), and calculated fracturing and hardness in boreholes (left) from chainage A1453. All images and parameters generated by Tunnel Manager.

From Figure 4.14 it is hard to see a clear resemblance with the engineering geological mapping. Very hard rock is registered in the beginning of the chainage, but according to the engineering geological mapping there is no evidence for harder rock except for at the end of the section where the drill bits may intersect a syenite dyke. The blue area in the hanging wall in the end of the chainage might reflect the syenite dyke. From looking at the images in Figure 4.14, it seems like the boreholes on the left side of the chainage are registering softer rock than the boreholes on the right side. In general the chainage seems to be heavy fractured except from one area at the right side of the beginning of the boreholes.

## 4.2.4 Chainage B1378

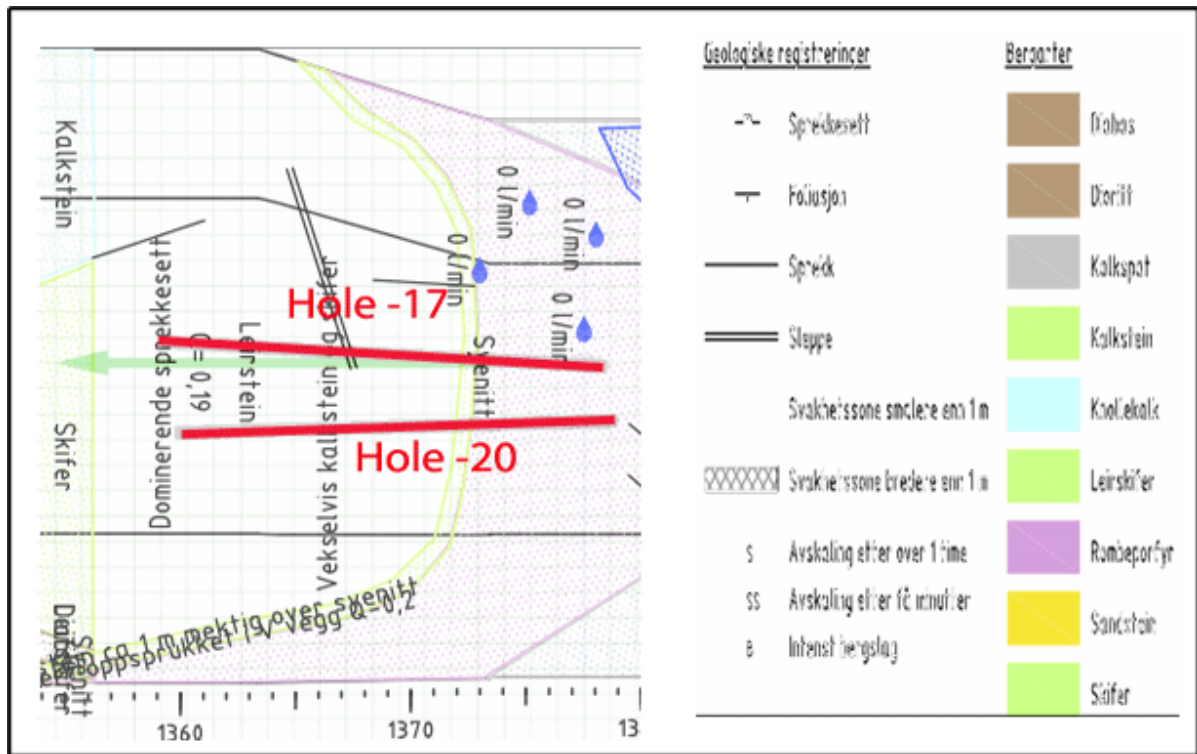
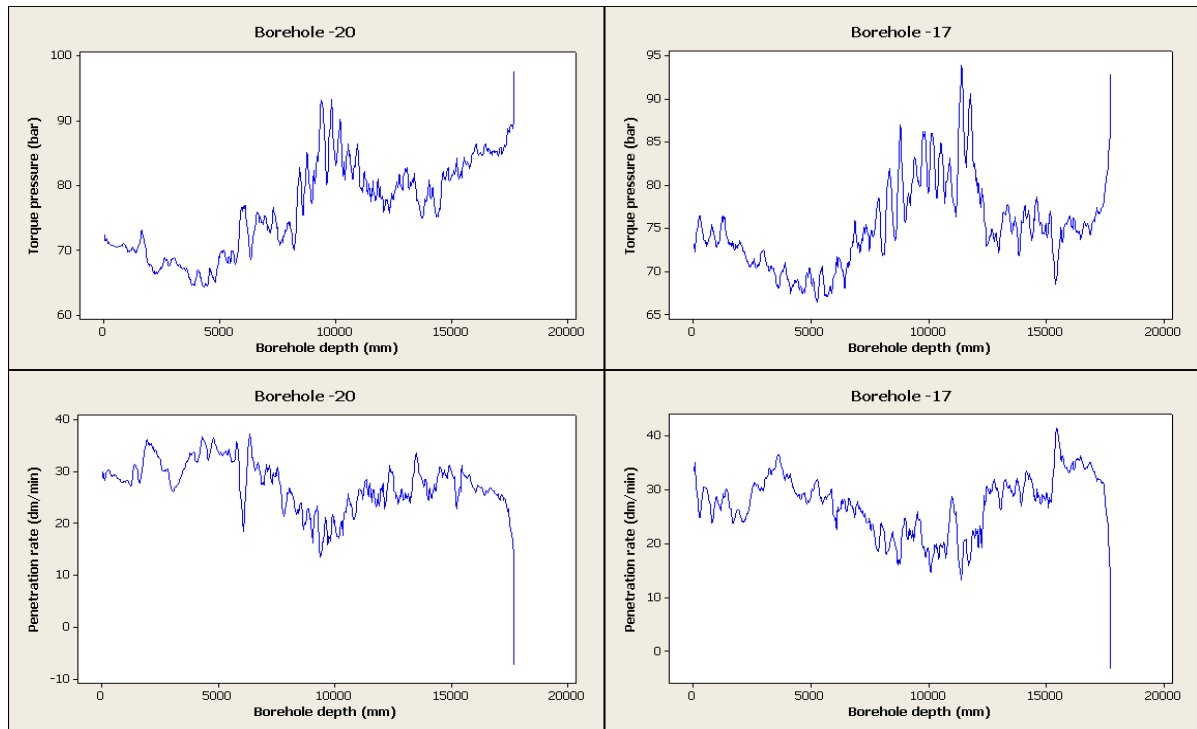


Figure 4.15. Location of boreholes -20 and -17. Section from chainage B1378.

Figure 4.15 show the location of boreholes -20 and -17 in chainage B1378. The boreholes start in syenite and continue into shale/claystone at approximately 6 meters borehole depth. Since the positioning of the holes are close together, and the boundaries between the two rock types are at the same depth for both holes, there are expected that the parameters for the different holes will correlate well to each other.



**Figure 4.16. Normalized torque pressure and penetration rate for chainage B1378, holes -20 and -17**

As seen in Figure 4.16, and as predicted, the plotted values do show resemblances. In general both torque pressure plots show a decreasing trend the first 5 meters borehole depth before the values increase. The general increase continues until approximately 10 meters borehole depth. At 15 meters borehole depth borehole -20 show an increasing trend in torque pressure, while the same interval in borehole -17 show a horizontal trend. The penetration rates for both boreholes show a negative trend from roughly 5 meters borehole depth until approximately 10 meters borehole depth. From borehole depth 10 meters and on, the general trend is positive for both holes.

In borehole -20, a negative peak in penetration rate is recorded at 6 meters borehole depth. At the same borehole depth, a positive peak is found in torque pressure. The highest torque pressure for borehole -20 coincides with the lowest penetration rate value (last reading in borehole neglected), and can be seen around borehole depth 9 meters. In borehole -17, at borehole depth around 3 meters a positive peak in penetration rate is recorded and a negative peak in torque pressure. The negative peak in torque pressure is not as distinctive as the positive one in penetration rate. At 11 meters borehole depth, the torque pressure shows a near vertical positive shift (from negative peak to positive peak), in penetration rate this is reflected by an opposite structure (from positive peak to negative peak). The negative peak in

torque pressure at 15,5 meters borehole depth is recorded as a positive peak in penetration rate.

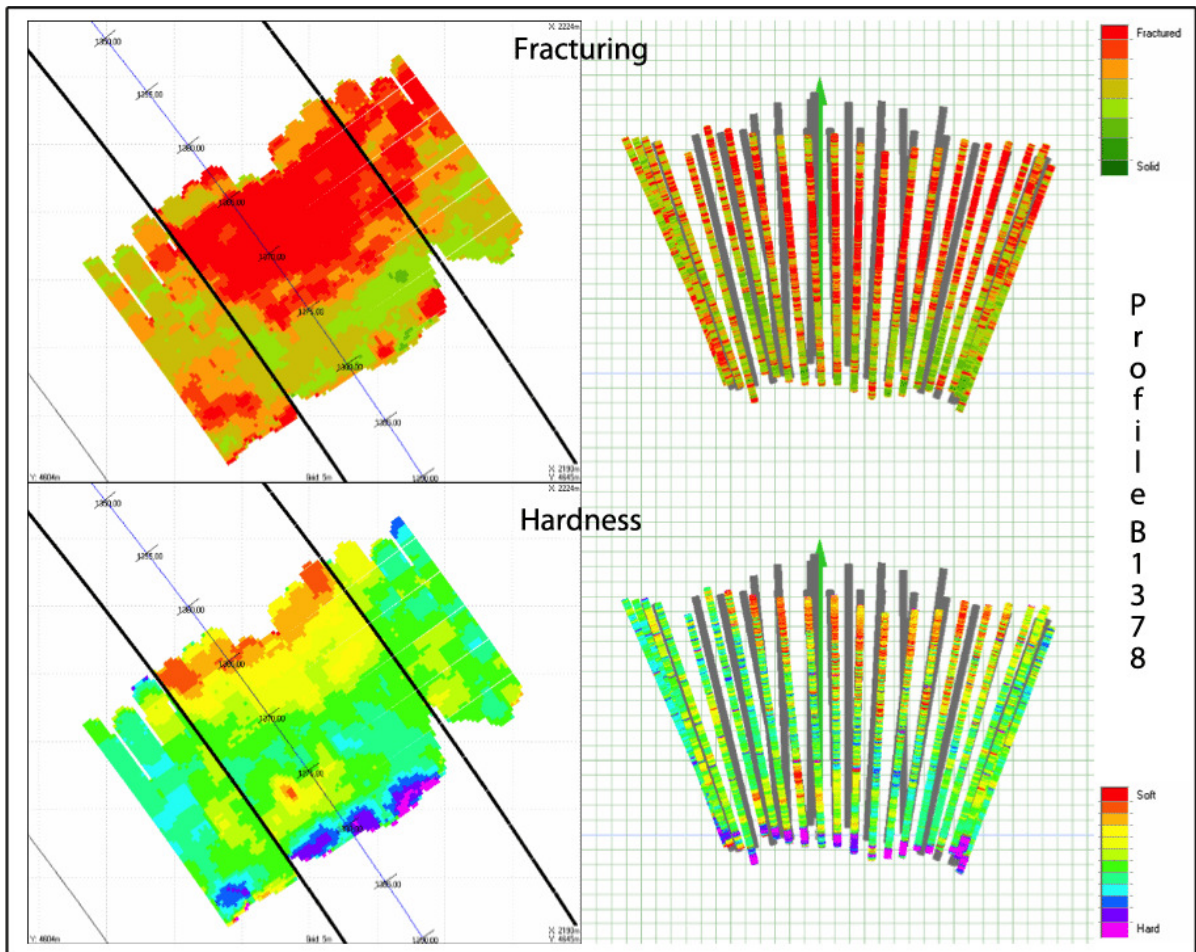


**Figure 4.17. Calculated fracturing and hardness mapping (left), and calculated fracturing and hardness in boreholes (left) from chainage B1378. All images and parameters generated by Tunnel Manager.**

From looking at the images in Figure 4.17 the shape of the syenite can be recognized both in the mapped hardness and the mapped fracturing. In this figure, as well as in Figure 4.11, Figure 4.8 and Figure 4.14 there are mapped zones of very hard rock at shallow borehole depths. From the engineering geological mapping we can see that there is not mapped any rock that is harder than the syenite in this area. And from looking at the above mentioned figures we can see that in general the syenite is mapped as green and light blue, not dark blue and purple.

## 4.2.5 Chainage B1476

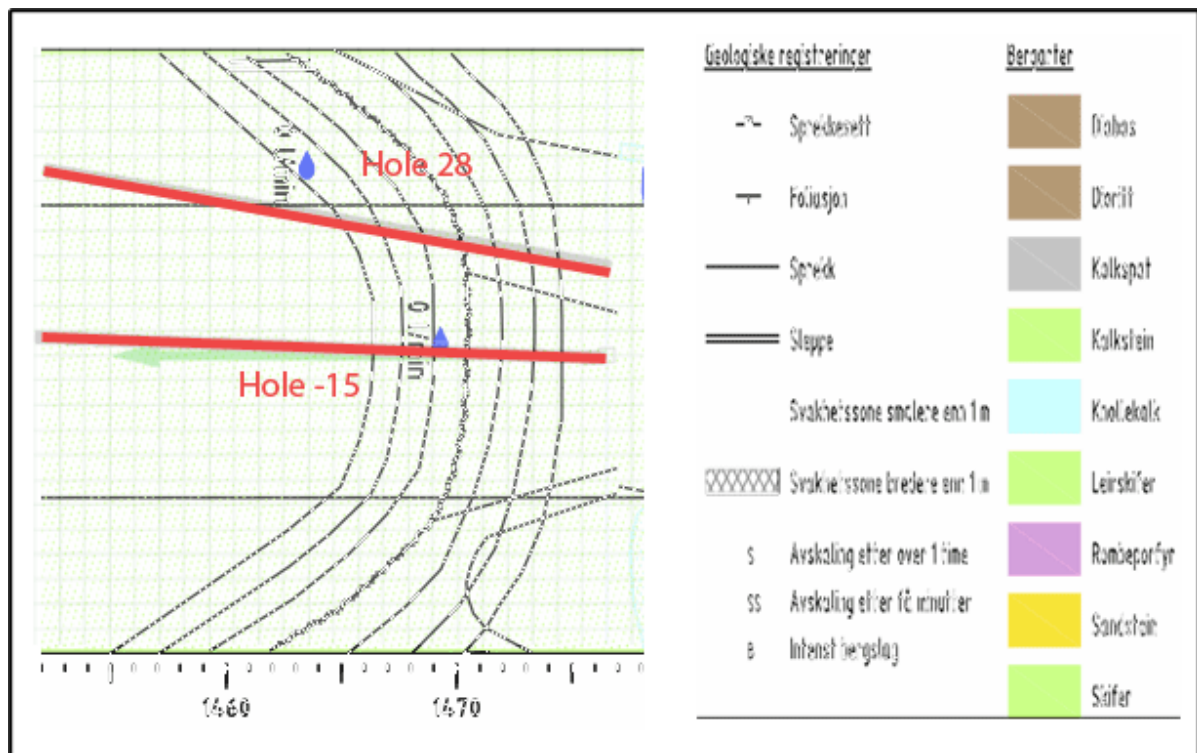
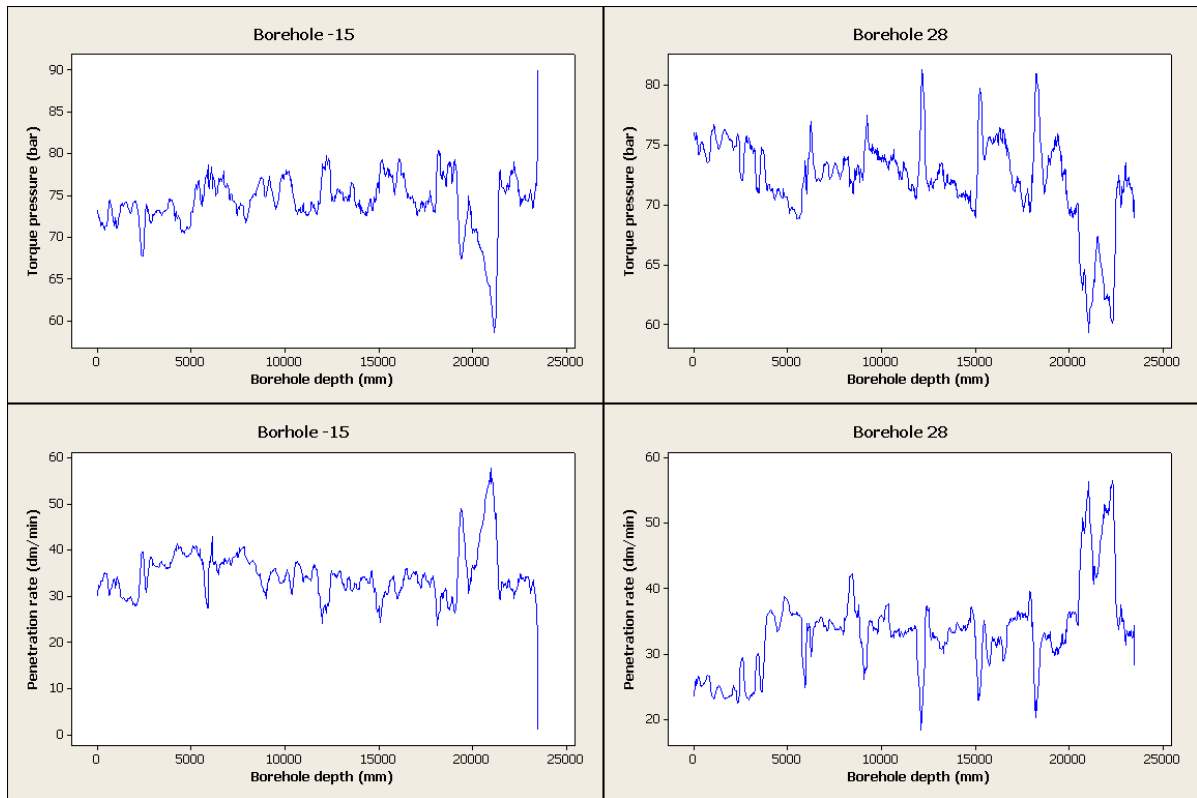


Figure 4.18. Location of boreholes -15 and 28. Section from chainage B1476.

Boreholes -15 and 28 are running through clay-shale during the entire drilling operation. They cross a zone of fractures after only a few meters. The fractures are expected to affect the parameters with a lot of variability; sudden peaks in both torque pressure and penetration rate. The deeper parts of the boreholes are expected to show less variation, thus no fractures or other geological features are mapped.



**Figure 4.19. Normalized torque pressure and penetration rate from chainage B1476, holes -15 and 28.**

As predicted from the engineering geological mapping, the penetration rates and torque pressures in boreholes -15 and 28 show close to horizontal trends (Figure 4.19). The variation in torque pressures and penetration rates in borehole -15 are fairly low in the range of 5 bar for torque pressure and 10 dm/min for penetration rate, except from the last 5 meters of the borehole where the variation is larger. At approximately 19 meters borehole depth a negative peak is recorded in torque pressure and a positive peak in penetration rate for borehole -15. At approximately 21 meters borehole depth the same response in parameters are recorded. In borehole 28 there are five positive peaks in torque pressure with approximately 3,3 meters between them. The first one is around 6 meters borehole depth. Five negative peaks are recorded in the penetration rate, with the same locations as the peaks in torque pressure. Around 21 and 23 meters borehole depth in borehole 28, it is recorded two negative peaks in torque pressure. In the same interval of penetration rates two positive peaks are registered.

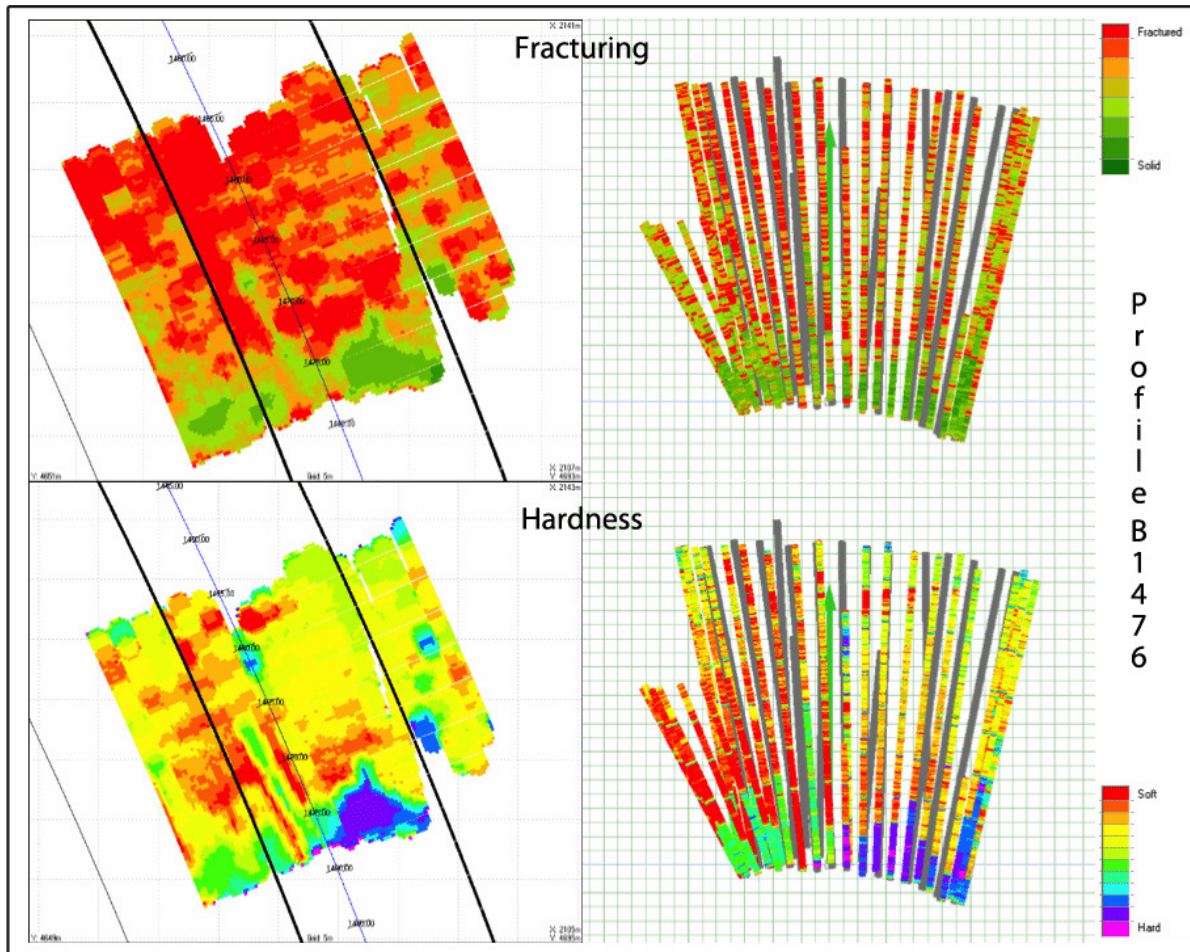


**Figure 4.20. Calculated fracturing and hardness mapping (left), and calculated fracturing and hardness in boreholes (right) from chainage B1476. All images and parameters generated by Tunnel Manager.**

The hardness mapping image in Figure 4.20 show a field of very hard rock in the centre of the hanging wall at the beginning of the borehole. Compared to the engineering geological mapping in Figure 4.18 it is hard to find evidence for this type of rock. The fracturing in the same area is marked as almost solid rock. The tendency of areas with harder rock early in the boreholes, which is seen in other sections mapped for hardness, are also seen here. In general the left side of the chainage seems like softer than the right side.

### 4.3 Tested rock hardness vs Penetration rate

From Table 3.1 we get both the UCS and Is50 strength of the different rocks found in the drill core samples. Theory of Kahraman et al. (2003) supports that the penetration rate correlates with the unconfined compressive strength.

**Table 4.4. Average penetration rate normalized for depth and UCS for syenite, limestone and shale**

	Syenite	Nodular Limestone	Shale
PR mm/min	33,2	42,0	45,4
UCS Mpa	178	45	36

In Table 4.4 the calculated averages of penetration rate and UCS of the rocks are shown. It seems clear that there are some relation between penetration rate and UCS as the values for syenite show that it is harder and has a lower average penetration rate. The relation of high UCS and low penetration rate is not reflected by the data from the shale and the nodular limestone. Here the penetration rate of the shale is lower than the penetration rate for nodular limestone, and the UCS is higher for the limestone than for the shale. The calculated averages can be found in *Appendix II*.

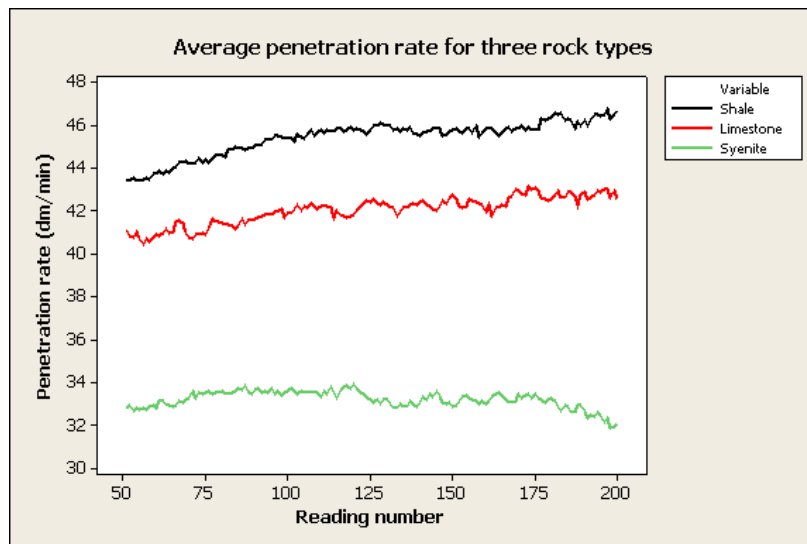


**Figure 4.21. Average blast borehole penetration rates for shale, limestone and syenite. Data are normalized for borehole depth.**

In Figure 4.21 the averaged penetration rate for the three selected rock types are presented. The average penetration rate for shale and limestone differ with about 1 dm/min, while the average penetration rate for syenite is around 8 dm/min lower than limestone.

## **5. Discussion**

### **5.1 The normalization process**

#### **5.1.1 General sensitiveness of normalization process**

As the normalization of borehole depth is based upon a regression analysis of averaged data it is clear that the amount of data has an important role on the validity of the normalization. In order to detect variations caused by other factors than geological structures, large datasets has to be averaged. The geology encountered in this thesis consists of different type of rocks, both sedimentary and igneous, crushed rock and fracture zones. The total amount of drill parameter data used to calculate regression lines is approximately 3000 injection boreholes and 10000 blast boreholes. However, these amounts of drill parameter data only reflect 440 meters of excavated tunnel in changing rock conditions. In Figure 4.1 and Figure 4.2, the difference between the injection boreholes and the blast boreholes are significant. While the blast borehole averages seem smooth (Figure 4.2) the injection borehole averages are more jagged. The jagged surface of the averaged injection boreholes would smoothen out if the amount of data was larger, and thus generate a trend more true to the machine affected signature and minimizing the effect from the varying geology.

#### **5.1.2 Normalization for borehole depth**

The averaged drill parameters plotted in Figure 4.1 show the distribution of data over borehole depth. To be sure that the regression line is chosen from data that reflects a general trend over borehole depth, it is important that the right amount of data is chosen. At the beginning of each borehole, the drill hammer does not drill at highest possible values. The result of the “soft” start will be a steep positive trend for the first meters of each borehole for penetration rate and feed thrust. These data are not representative for the general trends of the datasets, and has been removed in order to get a regression line that is representative for drilling parameters versus depth. However it could be discussed if another type of regression

fit could be assigned. The fit of a nonlinear regression could also be considered. But in general, the fact that the operator controlled parameters increase in the beginning of the borehole, somewhat hide the dependent parameters reflecting the geology.

To choose the low threshold, heuristic rules have been used. The threshold is chosen at the point where the increase of drill parameters stalls. A way to empirically choose a threshold could be to inspect the log from the control unit of the drill rig (Pers. com. Wetlesen, T. may 2010).

The high thresholds for injection boreholes are chosen at the point where the number of data that the calculated averages are based upon falls under a certain value (chapter 4.1.1). As the number of data used for the calculated average drops, the plotted averaged line increase in variation. This is clearly visible at the end of the plots in Figure 4.1. At the very last end of the average plots, the average is based upon only a few values, and thus the trend from machine settings are more abundant. However, heuristic rules are used here as well, and especially for the blast boreholes where the generated average plots extend to reading numbers higher than predicted.

During the last stage of this thesis, the python program was reprogrammed to write the number of values generated for the average. These data can be plotted against reading number to choose the correct threshold. This is seen in Figure 5.1 where a significant change in averaged data occurs at the average borehole length.

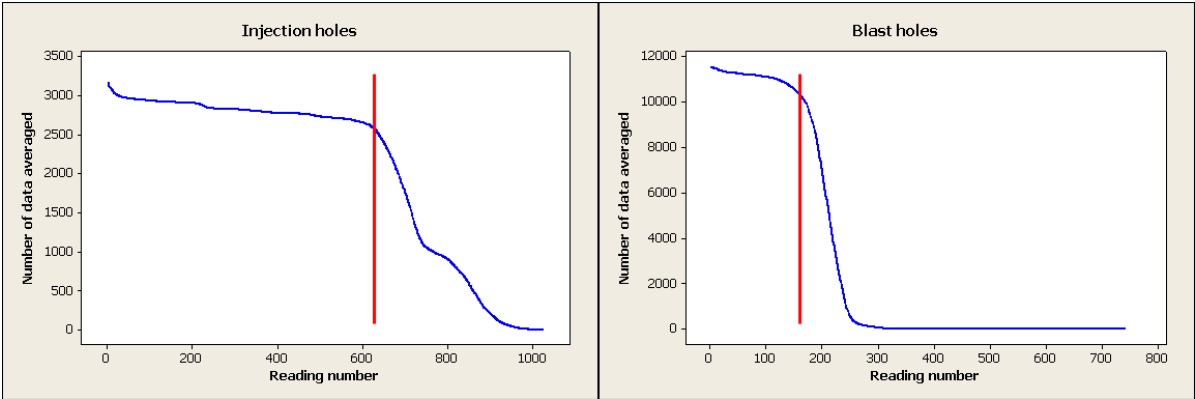


**Figure 5.1. Number of averaged data plotted against reading number. Red lines indicate the where the threshold should be placed regarding amount of data.**

The threshold chosen for injection boreholes in Figure 4.1 differ substantially, but would unlikely change the calculated regression line much. The threshold for blast boreholes seems more in place as the pre-chosen threshold not differ significantly from the one in Figure 5.1.

### 5.1.3 Normalization for feed thrust

The feed thrust highly affects the penetration rate and torque pressure (Schunnesson 1998). Normalization of penetration rate and torque pressure for feed thrust is therefore essential in order to obtain changes in geology instead of changes in feed thrust. One would predict an increase in both drilling parameters over increased feed thrust except at very high feed thrusts where the rotation of the drill bit will stall followed by a decrease in penetration rate.

The plots in Figure 4.3 show a LOWESS smoothing of the correlation between the parameters and the linear regression line. The majority of data is found around feed thrusts over 60 bar for injection boreholes and over 80 bar for blast boreholes. This is supported in Figure 4.1. As the majority of the data is found with low variation at high feed thrusts, outliers easily affect the calculated regression lines. However the data show good correlation values above 0,91 for all both penetration rate and torque pressures for both borehole types.

At shallow borehole depth thrust seems to be the parameter affecting torque pressure and penetration rate. It could be discussed if the data from the first meters of the borehole should be taken into account for normalizing for feed thrust. A possibility here would be to perform a separate normalization for shallow borehole depth for feed thrust.

### 5.1.4 Normalization for torque and penetration rate

The majority of the data show a fairly good correlation to each other except at high penetration rates and low torque pressures. In section 4.1.3 the data removed in order to get a valid trend line that represents the relationship between the two parameters as suggested by Schunnesson (Schunnesson 1998), has been described.

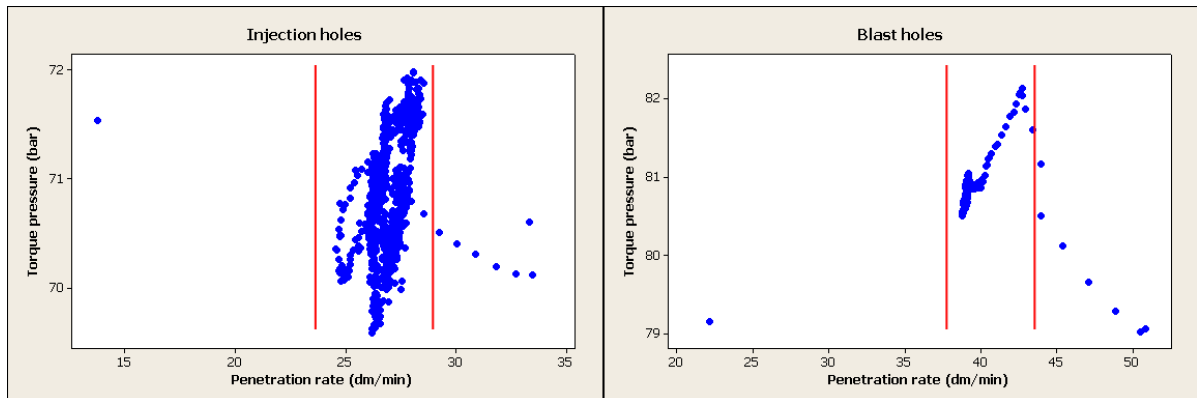


**Figure 5.2. Scatterplot of torque pressure and penetration rate with marked threshold. All data are normalized for borehole depth and feed thrust**

The data that has been removed as explained above are the data outside the red lines in Figure 5.2. The reduction of the dataset has major effects on the regression lines. From the plot it seems clear that the torque pressure show greater variability than the penetration rate. It can be discussed if the removal of data should have been done to a greater extent, especially for penetration rates above 39,3 dm/min for blast holes.

## 5.2 Discussion of geomechanical interpretation results

### 5.2.1 Chainage A1386

In borehole -53 (Figure 4.7) the torque pressure increases from approximately 5 to 10 meters borehole depth, before it suddenly decreases and stabilizes at around 90 bar. The penetration rate starts out fairly horizontal with a sudden decrease at 5 meters borehole depth. The low values of penetration rate lasts until borehole depth of 10 meters. A high torque pressure combined with low penetration rate could be a predicted response from a fracture zone or

lower rock hardness, but from the engineering geological mapping there is no such structure mapped in this area. Both torque pressure and penetration rate for both boreholes show low amount of variation after borehole depth of approximately 10 meters. In the Tunnel Manager generated mapping (Figure 4.8) a zone of softer rock is indicated at approximately 5 meters borehole depth, which correlates well to the distances in the boreholes. It could possibly be assumed that the penetration rates and torque pressures for the first meters of the borehole show somewhat distorted values, as the normalization process might not be sufficient to remove the signs from the “start up” of the drilling process, and in reality be much lower. As we don’t have data above the hanging wall except from drill parameters, we cannot now for sure where the drill bit intercepts the syenite, but it can be assumed that the marked rise in penetration rates at borehole depth 10 meters for borehole -53 indicate this boundary.

### **5.2.2 Chainage A1442**

At borehole depth 10 to 15 meters in borehole -58 in Figure 4.10 the penetration rate decreases over to sections around 2 meters thick. The same interval shows an increase in torque pressures. A decrease in penetration rate and increase in torque pressure could indicate fracturing zone (Schunnesson 1998). However, from looking at the engineering geological map, it seems obvious that the marked fracture zones are intercepted earlier than borehole depth 10 meters. The two syenite dykes crossing the tunnel section at chainage A1420 to A1430 would predict to intercept the borehole at approximately 10 meters. In the hardness mapping generated by Tunnel Manager, a zone of harder rock is mapped at approximately 8 meters borehole depth. As the hardness parameter in Tunnel Manager is supposedly closely correlated to penetration rate, it can be assumed that the syenite dykes are the structures affecting the penetration rate in borehole -58 and the hardness parameter in Tunnel Manager at around 10 meters borehole depth. From looking at the position of borehole 46 (Figure 4.9) it is most likely that the same structure will affect the penetration rate and torque pressure at a larger borehole depth. Borehole 46 shows a decrease in penetration rate and increase in torque pressure at around 10 meters borehole depth. Haug et al. (2007) discovered that the igneous rocks in the core drillings showed higher rate of fracturing than the sedimentary rocks in the cores. A high grade of fracturing along with high UCS values would predict low penetration rates and high torque pressure values. This supports the assumptions above, and it seems plausible to assume that the two shifts in both penetration rate and torque pressure are responses from the syenite dykes.

At the very beginning of the boreholes a fracture zone is mapped. At low borehole depth, both torque pressures are fairly high, thus might reflect the fracturing zone. The fact that the interval of high torque pressures is seen later in borehole 46 than in borehole -58 strengthens the assumption. However, the mapped fracturing parameters from Tunnel Manager do not show any particular signs of high fracturing in this area.

### **5.2.3 Chainage A1453**

Both torque pressure and penetration rate for borehole -17 (Figure 4.13) show fairly low variation along the borehole depth except from a section between 16 and 20 meters borehole depth, where the torque pressure decreases. A reduction in torque pressure could be seen in an area of harder rock along with a reduction in penetration rate. However it is unlikely that borehole -17 would cross the syenite dyke marked in the engineering geological mapping (Figure 4.12). At borehole depth of 18 meters the torque pressure is still low, but the penetration rate increases before it suddenly drops at 20 meters borehole depth. The rise in torque pressure at this borehole depth along with the negative peak in penetration rate may indicate that the drill bit has just reestablished rock contact after passing through a fracture. In the engineering geological mapping there is mapped a fracture zone in the area of 20 meters borehole depth. However, from the earlier assumptions it seems like the position of chainage numbers in the engineering geological mapping does not coincide with the chainage numbers gathered from the drill monitoring data, and that it is response from the fracture zone we can see in the drill parameters at approximately 16 meters depth. Borehole -14 has very high penetration rates at low borehole depth, but from Figure 4.12 it is hard to find evidence that supports the anomaly in penetration rate. As mentioned in section 5.2.1 this may be a weakness in the normalization process. The variations in penetration rate and torque pressure in interval 16 to 18 meters could possibly indicate a fracture zone, but again it is hard to find evidence that supports the assumptions from the engineering geological mapping. The hardness mapping from Tunnel Manager (Figure 4.14) does not correlate well to the engineering geological mapping, as it has calculated remarkably softer rocks on the left hand side of the chainage compared to the right side.

## 5.2.4 Chainage B1378

The two boreholes in chainage B1378 show good correlation to each other (Figure 4.16). The middle parts around borehole depth of 10 meters show high values of torque pressure and low values of penetration rates. As the boreholes start in a syenite dyke, lower penetration rates are expected along with lower torque pressures. In general the penetration rates in the boreholes in chainage B1378 are at fairly low values compared to the other boreholes, with average value below 30 dm/min. This supports the theory of lower drilling rates for harder rock. The increased penetration rates from borehole depth approximately 10 meters may indicate the boundary between the syenite and the shale. However the penetration rates for the first 7 to 8 meters of the borehole give no indication that harder rock is being drilled compared to the last part of the borehole. The low torque pressures however seem to match well to the theory of hard rock and low torque pressures. Compared to the hardness mapping from Tunnel Manager (Figure 4.17) the drill parameters correlate well. The shift in rock hardness has been calculated to about 10 meters in both the hardness mapping and normalized borehole parameters. The mapping of fractures show an increase in fracturing after approximately 7 meters depth, which is at the same borehole depth where the torque pressures start to increase.

## 5.2.5 Chainage B1476

Boreholes -15 and 28 are drilled through shale in the entire section (Figure 4.18), and large variations in penetration rate would not be expected. However there are marked several fractures the first 10 meters of the boreholes, and a variation in torque pressure could be expected. The variation of penetration rate for hole -15 is low for the entire borehole except from two peaks around 20 meters borehole depth. The torque pressure shows similarities with the penetration rate, but the peaks at high borehole depth are negative. The fracturing mapping from Tunnel Manager (Figure 4.20) show high levels of fracturing at the end of the section, and supports the assumptions drawn from the drill borehole parameters. At very shallow borehole depth, the hardness mapping has calculated the rock in an area to be hard. If compared to the hardness mapping in Figure 4.17, where the boreholes run through syenite, the color scaling indicate that the area consist of even harder rock than syenite.

In penetration rate, borehole 28, there are 5 negative peaks with approximately 3,3 meters interval. These peaks are most probably markers from the drill rod shifts, and can also be seen as positive peaks in the torque pressure plot.

### **5.2.6 Tested rock hardness vs penetration rate**

As predicted there is a clear difference between the penetration rate of syenite and the other two rock types. However, the nodular limestone show lower average penetration rate than the shale, all though the UCS for nodular limestone is higher (Table 4.4). The average data are based upon blast boreholes, and thus cannot be related to the penetration rates from injection holes. This is clearly visible in Figure 4.1 where we can see that the average penetration rate for injection boreholes is much lower than for blast boreholes. This is most likely a result of the lower feed thrust applied in injection boreholes to avoid drill rod deflection. As the geomechanical interpretation of drill parameters in this study are based upon injection holes, caution has been taking according to relating penetration rates from single boreholes towards rock hardness. It is however most likely that the relationship between UCS and penetration rate show the same relative difference for injection boreholes as blast boreholes.

There may be some pollutants since the data are chosen from the engineering geological mapping, and borehole data are from blasting holes which represents the whole excavated rock structure, and not only the roof and wall sections. Also, the accuracy of the positioning of the chainages differ from borehole data and engineering geological mapping. And it can be assumed that the data calculated for averages might contain other rock types than planned.

It would be both interesting and useful to investigate the average penetration rates for the other rock types discovered in the drill cores (Table 3.1), but at time of writing the amount of data available for other rock types than syenite, shale and limestone were limited. Especially penetration rate averages from the black shale, as it has the lowest UCS value of the tested rocks in the drill core, but only one section of approximately five meters thickness is mapped in the engineering geological mapping, and thus the extent of the rock type is to scarce to be predicted by the borehole data averages.

### 5.3 Remarks about collected drill monitoring data

During the final stages of the thesis, it has been known that there had been problems in the data acquisition from drill rigs (Pers. com. Stenerud, J. may 2010). The drill rigs were changed due to problems with sensors and reliable data were first collected at around chainage number 1440 to 1540. It is assumed that the problems mostly affected the drill parameters through missing data and not affecting the drill parameters significantly.

## 6. Conclusions

The main goals in this thesis were to see how well normalized drill parameters respond to changes in geology and how sensitive they are towards the normalization process along with the investigation of average penetration rates for different rock types.

In this thesis it was shown that:

- Wrong decisions could be taken if drilling data were to be analyzed without an initial normalization.
- The localization of geological boundaries could be done through inspecting normalized torque pressure and penetration rates.
- Rock types with different UCS values show different average non-normalized penetration rates.
- The normalization process for borehole depth is affected by the selection of thresholds.
- The normalization method presented seems to work fairly well, but show some weakness at shallow borehole depths.
- The normalization method is sensitive to outliers, especially for torque dependent penetration rate and vice versa.

## 7. References

- Andersen, T. 1998. Extensional tectonics in the Caledonides of southern Norway, an overview. *Tectonophysics* 285, 333-351.
- Goodman, R. 1989. *Introduction to Rock Mechanics*: John Wiley, Hoboken, NJ. 562 pp.
- Haug, R., Iversen, E. and Kveen, A. 2007. *Oppdrag A-37A Rapport nr. 3 Rv. 150 Lørentunnelen Geologisk rapport for konkurransegrunnlaget*. Oslo. Statens Vegvesen, Vegdirektoratet, 3.
- Honer, P.C. and Sherrell, F.W. 1977. The application of air-flush rotary percussion drilling techniques in site investigation. *Quarterly Journal of Engineering Geology and Hydrology* 10, 207-220.
- Hoseinie, S.H., Aghababaei, H. and Pourrahimian, Y. 2007. Development of a new classification system for assessing of rock mass drillability index (RDi). *Rock Mechanics and Rock Engineering* 45, 1-10.
- Howard, D.F., Adamson, W.R. and Berndt, J.R. 1986. Correlation of Model Tunnel Boring and Drilling Machine Performances with Rock Properties. *Int J Rock Mech Min Si & Geomech Abstr* 23, 171-175.
- Howarth, D.F. and Rowlands, J.C. 1987. Quantitative Assessment of Rock Texture and Correlation with Drillability and Strength Properties. *Rock Mechanics and Rock Engineering* 20, 57-85.
- Jimeno, C., Carcedo, F. and Jimeno, E. 1995. *Drilling and blasting of rocks*: Taylor & Francis. 389 pp.
- Kahraman, S., Bilgin, N. and Feridunoglu, C. 2003. Dominant rock properties affecting the penetration rate of percussive drills. *International journal of rock mechanics and mining sciences* 40, 711-723.
- Larsen, B.T., Olaussen, S., Sundvoll, B. and Heeremans, M. 2007. Vulkaner, forkastninger og ørkenklima. In Ramberg, I.B., Bryhni, I. and Nøttvedt, A. (eds). *Landet blir til, Norges geologi*: Norsk geologisk forening, 608.
- Liu, H. and Yin, K. 2001. Analysis and interpretation of monitored rotary blasthole drill data. *International Journal of Mining, Reclamation and Environment* 15, 177-203.
- Løset, F., Grimstad, E., Coughlin, P. and Kveldsvik, V. 1997. *Engineering Geology: Practical Use of the Q-Method*. Oslo. Norwegian Geotechnical Institute.
- NGU. *Berggrunnskart over Norge 2010* [Accessed: 26.05.2010. Available at <http://www.ngu.no/kart/bg250/>].

- Palmstrom, A. and Broch, E. 2006. Use and misuse of rock mass classification systems with particular reference to the Q-system. *Tunnelling and Underground Space Technology* 21, 575-593.
- Rabia, H. 1985. A unified prediction model for percussive and rotary drilling. *Mining Science and Technology* 2, 207-216.
- Schunnesson, H. 1996. RQD predictions based on drill performance parameters. *Tunneling and Underground Space Technology* 11, 345-351.
- Schunnesson, H. 1997. *Drill process monitoring in percussive drilling for location of structural features, lithological boundaries and rock properties, and for drill productivity evaluation*, Department of Environmental Planning and Design Division of Applied Geology, Luleå University of technology, Luleå.
- Schunnesson, H. 1998. Rock characterisation using percussive drilling. *International journal of rock mechanics and mining sciences*(1997) 35, 711-725.
- Scoble, M., Peck, J. and Hendricks, C. 1989. Correlation between rotary drill performance parameters and borehole geophysical logging. *Mining Science and Technology* 8, 301-312.
- Sinkala, T. 1991. Relating drilling parameters at the bit-rock interface: theoretical and field studies. *Mining Science and Technology* 12, 67-77.
- Statens\_Vegvesen. *Lørentunnelen - fra Økern til Sinsen* 2009 [Accessed: 14.01.2010]. Available at <http://www.vegvesen.no/Vegprosjekter/Ring3/Lørentunnelen>.
- Thuro, K. 1997. Drilability prediction: geological influences in hard rock drill and blast tunnelling. *Geol Rundsch* 86, 426-438.
- Tsoutrelis, C. 1969. Determination of the compressive strength of rock in situ or in test blocks using a diamond drill, 311-312.
- Yue, Lee, Law and Tham. 2003. Automatic monitoring of rotary-percussive drilling for ground characterization - illustrated by a case example in Hong Kong. *International journal of rock mechanics and mining sciences*(2004) 41, 573-612.

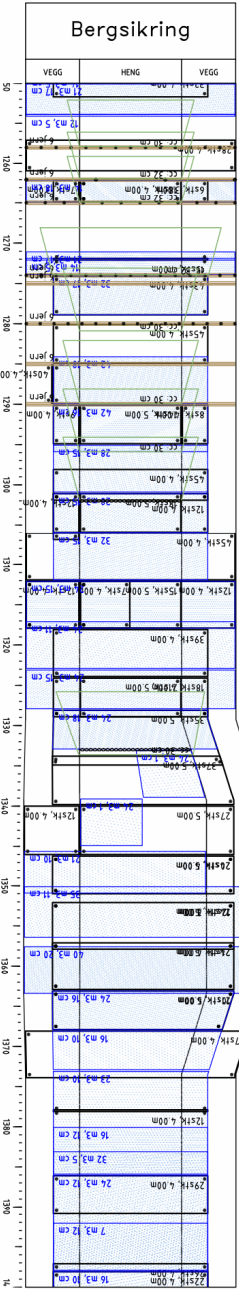
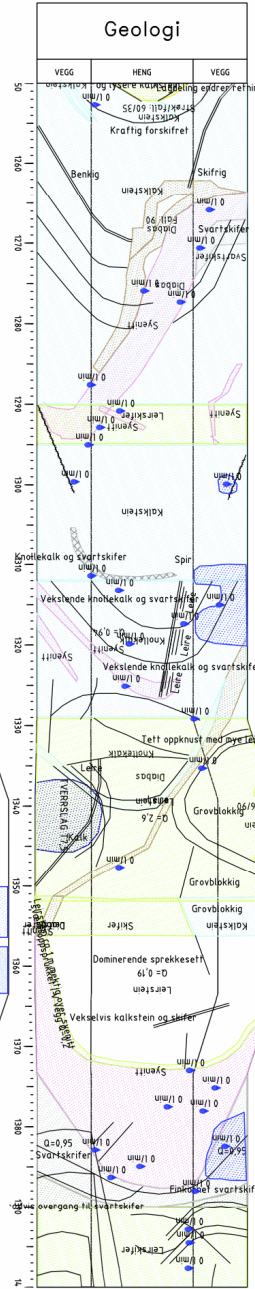








Bygning	1	2	3	4	5	6	7	8	9	10	11	12	13	14	15	16	17	18	19	20	21	22	23	24	25	26	27	28	29	30	31	32	33	34	35	36	37	38	39	40	41	42	43	44	45	46	47	48	49	50	51	52	53	54	55	56	57	58	59	60	61	62	63	64	65	66	67	68	69	70	71	72	73	74	75	76	77	78	79	80	81	82	83	84	85	86	87	88	89	90	91	92	93	94	95	96	97	98	99	100
Bygning	1	2	3	4	5	6	7	8	9	10	11	12	13	14	15	16	17	18	19	20	21	22	23	24	25	26	27	28	29	30	31	32	33	34	35	36	37	38	39	40	41	42	43	44	45	46	47	48	49	50	51	52	53	54	55	56	57	58	59	60	61	62	63	64	65	66	67	68	69	70	71	72	73	74	75	76	77	78	79	80	81	82	83	84	85	86	87	88	89	90	91	92	93	94	95	96	97	98	99	100
Bygning	1	2	3	4	5	6	7	8	9	10	11	12	13	14	15	16	17	18	19	20	21	22	23	24	25	26	27	28	29	30	31	32	33	34	35	36	37	38	39	40	41	42	43	44	45	46	47	48	49	50	51	52	53	54	55	56	57	58	59	60	61	62	63	64	65	66	67	68	69	70	71	72	73	74	75	76	77	78	79	80	81	82	83	84	85	86	87	88	89	90	91	92	93	94	95	96	97	98	99	100
Bygning	1	2	3	4	5	6	7	8	9	10	11	12	13	14	15	16	17	18	19	20	21	22	23	24	25	26	27	28	29	30	31	32	33	34	35	36	37	38	39	40	41	42	43	44	45	46	47	48	49	50	51	52	53	54	55	56	57	58	59	60	61	62	63	64	65	66	67	68	69	70	71	72	73	74	75	76	77	78	79	80	81	82	83	84	85	86	87	88	89	90	91	92	93	94	95	96	97	98	99	100



**Beregning**

- Kombinasjonsstøpe, vedboksstøf
- Enderettede, vedboksstøf
- Andre støpetyper, vedboksstøf
- ▭ Formbet
- ▭ Strømsbet
- ▭ Sprøytebetong
- ▭ Utsteining
- ▭ Fyllbunn
- ▭ Strømsgrøft
- ▭ Inneksjon

**Geotekniske registreringer**

- ▭ Sprekkeseff
- ▭ Falsisjon
- ▭ Sprekk
- ▭ Steppe
- ▭ Støttestone bredere enn 1 m
- ▭ Støttestone bredere enn 1 m
- ▭ Askekløst etter 1 time
- ▭ Askekløst etter 10 minutter
- ▭ Intert bergslag

**Beregnet**

- ▭ Diabas
- ▭ Dørrtt
- ▭ Kalkstein
- ▭ Knøttelek
- ▭ Kvarstitt
- ▭ Lærstein
- ▭ Sandstein
- ▭ Skifer

**Vann**

- ▭ Lekasje, punkt
- ▭ Lekasje, områdemerke

**Beregnet**

- ▭ A - Svartskiferstrøm god (4.0-10.0)
- ▭ B - God (10-4.0)
- ▭ C - Middels (4.-10)
- ▭ D - Dårlig (1-4)
- ▭ E - Svært dårlig (0.-1)
- ▭ F - Ekstremt dårlig (0.01-0.1)
- ▭ G - Eksplosivt dårlig (0.01-4.0)
- ▭ Ikke kontrollert med Q-verdi

Bygning	1	2	3	4	5	6	7	8	9	10	11	12	13	14	15	16	17	18	19	20	21	22	23	24	25	26	27	28	29	30	31	32	33	34	35	36	37	38	39	40	41	42	43	44	45	46	47	48	49	50	51	52	53	54	55	56	57	58	59	60	61	62	63	64	65	66	67	68	69	70	71	72	73	74	75	76	77	78	79	80	81	82	83	84	85	86	87	88	89	90	91	92	93	94	95	96	97	98	99	100
Bygning	1	2	3	4	5	6	7	8	9	10	11	12	13	14	15	16	17	18	19	20	21	22	23	24	25	26	27	28	29	30	31	32	33	34	35	36	37	38	39	40	41	42	43	44	45	46	47	48	49	50	51	52	53	54	55	56	57	58	59	60	61	62	63	64	65	66	67	68	69	70	71	72	73	74	75	76	77	78	79	80	81	82	83	84	85	86	87	88	89	90	91	92	93	94	95	96	97	98	99	100
Bygning	1	2	3	4	5	6	7	8	9	10	11	12	13	14	15	16	17	18	19	20	21	22	23	24	25	26	27	28	29	30	31	32	33	34	35	36	37	38	39	40	41	42	43	44	45	46	47	48	49	50	51	52	53	54	55	56	57	58	59	60	61	62	63	64	65	66	67	68	69	70	71	72	73	74	75	76	77	78	79	80	81	82	83	84	85	86	87	88	89	90	91	92	93	94	95	96	97	98	99	100
Bygning	1	2	3	4	5	6	7	8	9	10	11	12	13	14	15	16	17	18	19	20	21	22	23	24	25	26	27	28	29	30	31	32	33	34	35	36	37	38	39	40	41	42	43	44	45	46	47	48	49	50	51	52	53	54	55	56	57	58	59	60	61	62	63	64	65	66	67	68	69	70	71	72	73	74	75	76	77	78	79	80	81	82	83	84	85	86	87	88	89	90	91	92	93	94	95	96	97	98	99	100



## Appendix II: CD

### Contents:

- Python program for calculated averages
- Calculated averages of blast and injection holes
- Calculated averages of selected rock types
- Normalization process, spreadsheets
- Normalized borehole data, spreadsheets